A Tale of Three LPAs: Some Notes on Zig-Zag Log-Periodic Arrays
1. Preliminaries and LPDAs

L. B. Cebik, W4RNL

In amateur radio literature on log-periodic arrays (LPAs), an interesting situation has arisen. One of the many types of LPAs, the log-periodic dipole array (LPDA), has supplanted all other types. Today, literature generally available to amateurs (with one exception) overlooks other types of wire-based LPAs and provides detailed design information only on the LPDA. That situation naturally aroused my curiosity. How well or poorly did other types of LPAs perform relative to the easily modeled LPDA?

Two configurations of LPAs that were cotemporary with the earliest LPAs used structures that the average builder might reasonably replicate: trapezoidal elements and saw tooth elements in a zig-zag arrangement. Therefore, we obtain a 3-way comparison that gives us our title, a tale of three LPAs. However, the situation is not as simple as this, since we find versions that use a central boom and versions without the boom. Hence, we end up with the 5 varieties shown in **Fig. 1**.

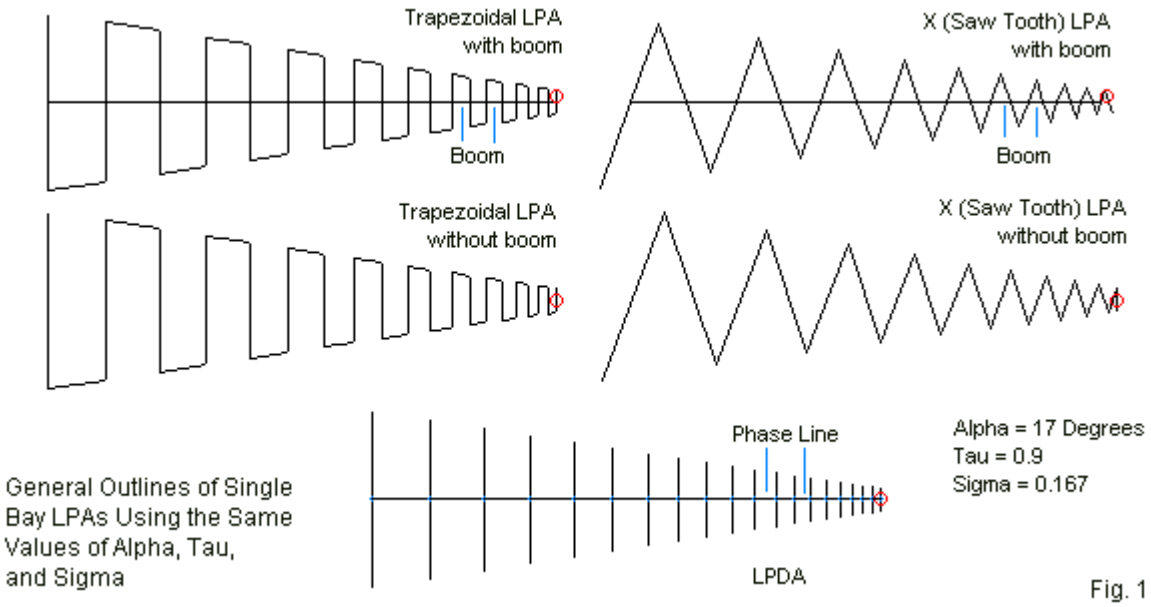

Fig. 1

Next, we add in a second complication. Normally, we find the LPDA, composed of dipole elements with a central 2-wire phase line transposed between each adjacent element, used in single bays. However, to make a directional array from any of the zig-zag forms, we need two bays, since the feedpoint is single-ended for a 1-bay version. In use, the 2-bay zig-zag LPAs show an angle between the bays in the H-plane. Therefore, all of the zig-zag arrays, whether using trapezoidal or saw-tooth elements, have a 3-dimensional structure, as shown in **Fig. 2**. The sample zig-zag arrays show only boomless versions for clarity. We might have as easily, but less clearly, used zig-zag LPAs with booms. The side and top view of the saw-tooth version of the zig-zag array shows us how the array developed the “X” designation.

By comparison, we may consider the single-bay LPDA to be a 2-dimensional structure. Nothing in the theory of LPDA development precludes the use of multiple bays, and some

commercial examples do exist. In developing our comparisons, we shall want to examine at least 2-bay LPDAs to improve the scope of our comparisons. One critical variance between 2-bay zig-zag LPAs and 2-bay LPDAs is a difference in how we feed the bays. Zig-zag arrays will require a single series feed between the bays, while 2-bay LPDAs will require parallel in-phase feeding.

Fig. 2

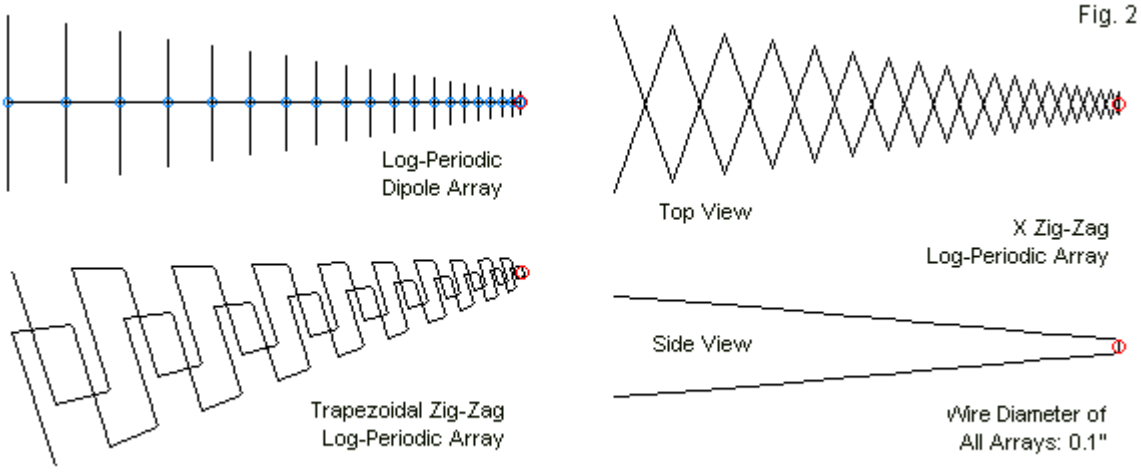

A Family of Log-Periodic Arrays

We also need to find a common set of standards for the design of each array so that all versions used in comparisons are in fact comparable. Setting aside the general tendency to try to obtain the greatest performance from the least wire, we shall use fairly long-boom versions of the arrays. Each array will use 20 elements per bay with design values that yield no anomalous frequencies across a 50-200-MHz passband. To avoid pressing NEC modeling limitations within the passband, all LPAs will use 0.1”-diameter (2.54-mm) lossless wire.

For various reasons that will become clear as we progress, the comparisons will require that we take relatively small and orderly steps. In this part of our journey, we shall look at some basic differences between the ways in which zig-zag and LPDA arrays are designed in classical terms. In addition, since the LPDA is the modern standard LPA for radio amateurs, we shall set up some base-line data for both single-bay and double-bay versions of the antenna. In part 2, we shall survey trapezoidal zig-zag arrays including versions with and without booms. Part 3 will look at the X or saw tooth configuration of the zig-zag LPA, again including versions with and without booms. The exercise has yielded a very large collection of NEC-4 modeling data, far too much for inclusion in the main text of these notes. Therefore, I shall make available a data appendix containing tabular and graphical information derived from each variation of each LPA that we consider. At 45 pages, the data appendix will be almost as long as all three parts of these notes combined.

Some LPA Background and Design Considerations

We may consider the years between the late 1950s and about 1970 as the period of peak development in log periodic frequency-independent antennas. Earlier work exists and later developments have improved the state of the art, but the indicated period was perhaps the most productive. Much of the work emerged from the Antenna Lab at the University of Illinois (Champagne-Urbana) or from the students and faculty after leaving Illinois. Paul Mayes kindly provided me with a copy of his 1982 article, “Frequency-Independent Antennas: Birth and

Growth of an Idea," which appeared in the August issue of the *Antennas and Propagation Society Newsletter* of the IEEE. One may track the contents of this brief history of developments by reading in chronological order the references in Chapter 14 of the third edition of Johnson's *Antenna Engineering Handbook*. Since our interests lie in wire-outline versions of the LPA, we may pass over the fundamental work on conical log-periodic antennas and focus more directly on linear antennas.

We may call our subject LPAs wire-outline arrays because they ultimately derived from solid element versions. For example, we may picture the zig-zag bays in **Fig. 1** as if each "tooth" consisted of a solid surface of conductive material. Early tooth designs assumed many shapes, many with curved structures that remind us that the LPA is based on limited arcs of a circle. The discovery that straight elements did not significantly reduce performance potential led to the substitution of wire outlines for the solid teeth. The counterpart of the boom in these early LPAs also increased in width as one moved from the vertex outward to the longest element. Shrinking the boom to a single wire led J. W. Carr to remove the boom altogether and still obtain a workable LPA. Hence, we have the potential for both boomed and boomless zig-zag LPAs, although in practice, only the X-array received much attention. Around 1970, I built a simple boomless X LPA as an attic television antenna that served well to improve reception in Athens, GA, from the network Atlanta stations about 70 miles distant.

In its most basic form and in terms that precede those we commonly use for LPDAs, the zig-zag LPA requires attention to only 3 terms: τ, α, and ψ. **Fig. 3** gives us a basic orientation to the meanings of these terms.

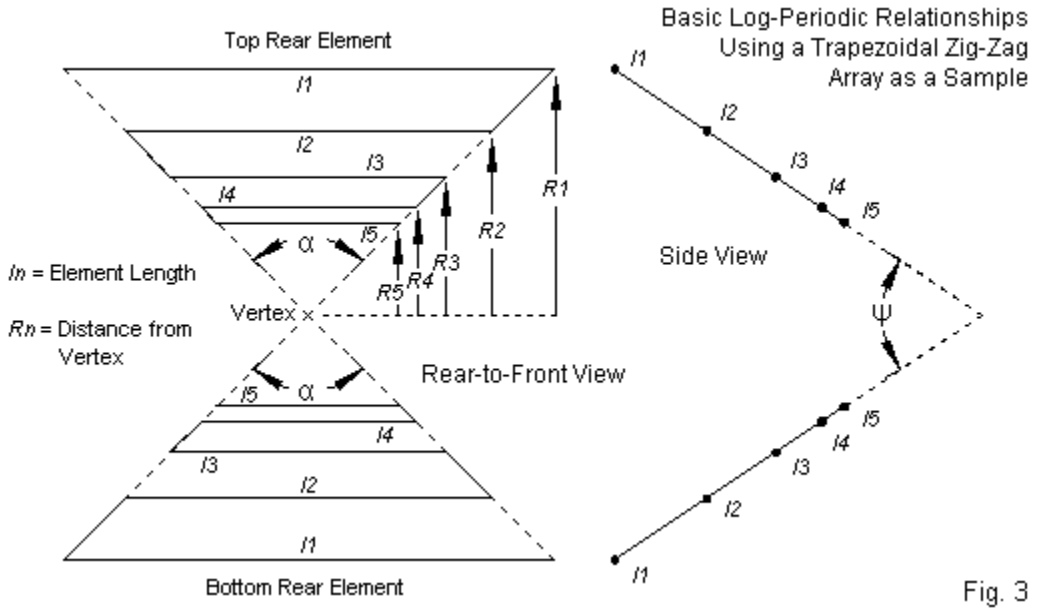

Fig. 3

The series of elements in the sketch have lengths and a distance from the vertex of the angles determined by the value of τ. We may define τ in terms of the element lengths (L), the distances from the vertex (R), or the spacing between elements (D):

$$\tau = \frac{R_{n+1}}{R_n} = \frac{D_{n+1}}{D_n} = \frac{L_{n+1}}{L_n}$$

We use the designation R for the distance from the vertex because each element is a straight-line distortion of what should in principle be an arc. However, the arc sections are too small to notice the distortion.

The distance from the longest element to the vertex depends upon its length. For this exercise, I have cut the element to be a physical half-wavelength at the lowest operating frequency. In practice, this element might be advisably somewhat longer. However, the slightly deficient longest element will be serviceable to our comparisons, since we may compare the degree of decrease in performance at the low end of the passband within the scans for each LPA. Once we know the length of the longest element, the distance to the vertex, R_V, is a simple tan function:

$$R_V = \frac{0.5\,L_1}{\tan(0.5\alpha)}$$

Note that determining the distance requires that we select the angle α (as designated in **Fig. 3**). At this point we encounter a difference between designations used for zig-zag designs and for LPDAs. For zig-zag designs, α is the total angle from one edge of the array to the other. As shown in **Fig. 4**, LPDAs nowadays define α as the angle from the centerline of the array to either virtual edge line. To avoid confusion in the immediately following notes, I shall re-designate the zig-zag angle as α'.

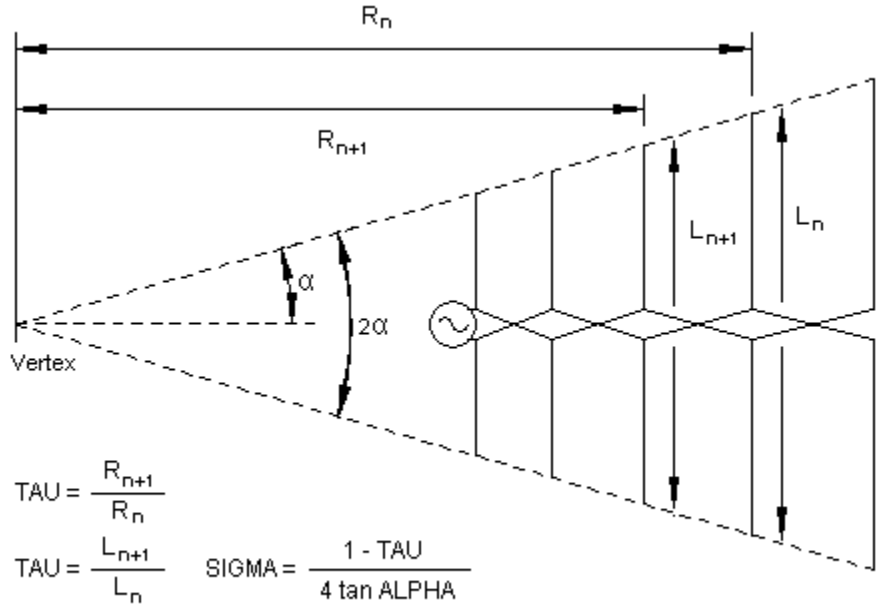

Log-Periodic Basics Applied to Dipole Arrays Fig. 4

Unlike design procedures for LPDAs, zig-zag designs normally calculate element (L) and spacing (R) dimensions by reference solely to τ and to α'. The length of element 2 is τ times the length of element 1. The distance from the vertex to the position of element 2 is τ times R_V. When we are done adding elements, the array boom length is simply R_V - R_n, where n is the most forward element. The procedure is simple enough to admit of an equally simple spreadsheet. **Fig. 5** provides a sample, with the dimensional values that we shall eventually employ in NEC-4 models of the three types of LPAs. Note that the worksheet has an entry marked "L*1.6." This is the length of an element with a resonant frequency that is 1.6 times the

highest operating frequency. This practice follows general guidelines for effective LPDA design, but it may prove to be a limiting factor for at least some zig-zag designs.

Zig-Zag Log-Periodic Antenna Elements											Fig. 5
Work Sheet		**Bold = User Entry**									
Tau		**0.90**								Sigma	0.167
Alpha'	degrees	**17.00**	degrees	0.297	radians	1/2Alpha'	0.148	tanAlpha	0.1495		0.167
F-low		**50.00**	MHz								
F-high		**200.00**	MHz								
L-long		3.00	meters	9.84	feet	118.11	inches				
Lhigh		0.75	meters	2.46	feet	29.53	inches				
L*1.6		0.47	meters	1.54	feet	18.45	inches				
Rv	Vertex R	10.04	meters	32.93	feet	395.15	inches				
Element	Ln	Ln/2	Rn	Element	Lfeet	Lft/2	Rfeet	Element	Linch	Lin/2	Rinch
1	3.00	1.50	10.04	*1*	9.84	4.92	32.93	*1*	118.11	59.06	395.15
2	2.70	1.35	9.03	*2*	8.86	4.43	29.64	*2*	106.30	53.15	355.63
3	2.43	1.22	8.13	*3*	7.97	3.99	26.67	*3*	95.67	47.83	320.07
4	2.19	1.09	7.32	*4*	7.18	3.59	24.01	*4*	86.10	43.05	288.06
5	1.97	0.98	6.59	*5*	6.46	3.23	21.60	*5*	77.49	38.75	259.26
6	1.77	0.89	5.93	*6*	5.81	2.91	19.44	*6*	69.74	34.87	233.33
7	1.59	0.80	5.33	*7*	5.23	2.62	17.50	*7*	62.77	31.38	210.00
8	1.43	0.72	4.80	*8*	4.71	2.35	15.75	*8*	56.49	28.25	189.00
9	1.29	0.65	4.32	*9*	4.24	2.12	14.17	*9*	50.84	25.42	170.10
10	1.16	0.58	3.89	*10*	3.81	1.91	12.76	*10*	45.76	22.88	153.09
11	1.05	0.52	3.50	*11*	3.43	1.72	11.48	*11*	41.18	20.59	137.78
12	0.94	0.47	3.15	*12*	3.09	1.54	10.33	*12*	37.06	18.53	124.00
13	0.85	0.42	2.83	*13*	2.78	1.39	9.30	*13*	33.36	16.68	111.60
14	0.76	0.38	2.55	*14*	2.50	1.25	8.37	*14*	30.02	15.01	100.44
15	0.69	0.34	2.30	*15*	2.25	1.13	7.53	*15*	27.02	13.51	90.40
16	0.62	0.31	2.07	*16*	2.03	1.01	6.78	*16*	24.32	12.16	81.36
17	0.56	0.28	1.86	*17*	1.82	0.91	6.10	*17*	21.89	10.94	73.22
18	0.50	0.25	1.67	*18*	1.64	0.82	5.49	*18*	19.70	9.85	65.90
19	0.45	0.23	1.51	*19*	1.48	0.74	4.94	*19*	17.73	8.86	59.31
20	0.41	0.20	1.36	*20*	1.33	0.66	4.45	*20*	15.95	7.98	53.38

Basic zig-zag design procedures do not require the term σ, which LPDAs depend upon for more than one step in the design procedure. We may derive σ from α and τ in LPDA terms:

$$\sigma = \frac{1-\tau}{4\tan\alpha} = \frac{D_n}{2L_n}$$

Most LPDA design literature recommends the use of the optimal values for σ:

$$\sigma_{opt} = 0.243\tau - 0.051$$

In fact, many zig-zag designs employ values of what I shall call virtual σ that are close to optimal. Where the literature seems oddest is in the occasional use of very low values of τ. LPDA design recommends the use of values above 0.8—and considerably higher if feasible. However, we may commonly find τ values from 0.6 to 0.7 in some zig-zag designs. The modeled performance of some zig-zag designs using low values of τ eventually led to the use of 0.9 in the three models that we shall compare. See **Fig. 5** for a visual account of why low values of τ produce less than optimal results.

The three patterns all use the same values of α' (60°) and of ψ (35°) for a trapezoidal zig-zag LPA with a 50-200-MHz design range. (We shall examine ψ momentarily.) As we increase the value of τ, the sidelobes diminish. However, as we reach a τ of 0.9, the pattern degrades in a different manner, with a broader main lobe—almost a double lobe to match the enlarged rear

quartering lobes. This pattern results from the use of a value of α' much larger than is optimal for the value of τ.

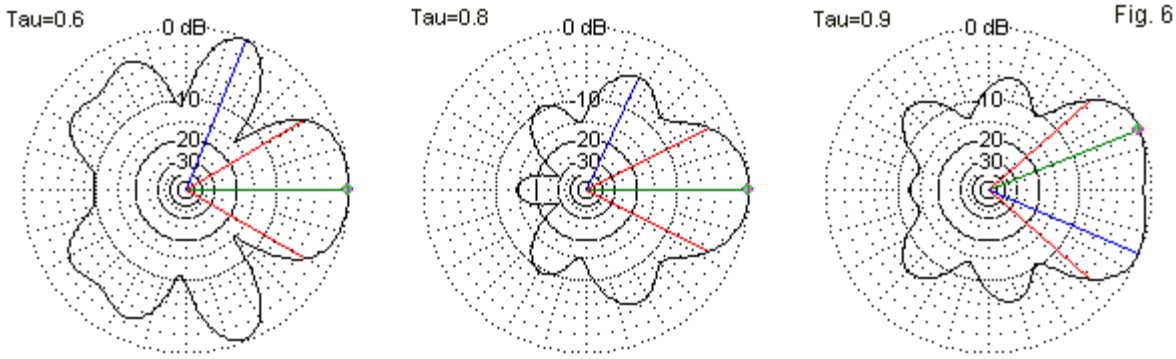

Fig. 6

All E-plane patterns are for 150 MHz, with Alpha = 60 degrees and Psi = 35 degrees.

Sample Free-Space E-Plane Patterns of Trapezoidal Zig-Zag LPAs Using Low Values of Tau

By using a selected value of τ, we may calculate the optimal value of σ from LPDA design recommendations. Next, we may back-calculate, using the recommended value of σ_{opt}, the corresponding value of α':

$$\alpha'_{opt} = 2\tan^{-1}\left(\frac{1-\tau}{4\sigma}\right)$$

For a τ of 0.9, the optimal value of σ is about 0.1677. The corresponding value of α' is very close to 17°. The worksheet in **Fig. 5** shows the entries for α' and τ, along with the calculated value of virtual σ as a check.

As shown in **Fig. 3**, zig-zag LPAs require two bays separated by an angle designated ψ. Early designs favored relatively wide angles or high values of ψ. As we increase the value of ψ, the gain increases but the front-to-back ratio decreases. As a consequence, designers settled on a value for ψ experimentally, arriving at a compromise that best fit the research or communications application at hand. Since the rates of change of gain and of the front-to-back ratio are not constant at all frequencies within the operating range, there is no clear mathematical relationship between the values of α' and ψ. However, in a broad sense, we may note in advance that the two angles are related so that decreases in the value of α' result in decreased values for ψ. To establish that fact for both trapezoidal and X versions of zig-zag LPAs, we shall have to explore samples in Part 2 and 3 of these notes.

The exploration will employ NEC-4 models in free space using 0.1"-diameter lossless or perfect wire. Modeling the elements for any type of LPA is routine with one exception. If we multiply each value for R by –1, we obtain an X-coordinate for the element's position. This procedure offsets the array from the coordinate system center in accord with the calculated value of R_V, the distance of the element to the vertex of the array. Then we may rotate the bay on the Y-axis using either an interface facility in the program (such as EZNEC Pro/4) or via the GM command. As well, we need model only a single bay, since we may replicate that bay and rotate the replica 180° on the X-axis. I have used a simple feedpoint system of running a wire from the free ends of the two most forward elements. Experiments that extended wires to the vertex produced no significant changes in the basic array performance, so I settled on the simpler feedpoint modeling procedure.

Segmenting NEC models of an LPA with a significant frequency range (in this case, 4:1) generally require a compromise between adequate segmentation and model size. Ideally, the segment length should be about 0.05-λ at the highest frequency used. Maintained this segmentation density requires inverse τ-tapering of the number of segments per element as we proceed from the vertex toward the longest element. Of course, the number of segments is an integer, with consequential rounding. In an LPDA, the segment count must also be an odd number to place the modeled phase line (a transmission line using NEC's TL facility) at the element center. Since the models are committed to a uniform wire diameter throughout (rather than using τ-tapered element diameters), there is a limit to the level of segmentation, since that is determined by the wavelength at a frequency about 1.6 times the highest frequency in the passband. It is fairly easy to exceed recommended ratios between the wire radius and the segment length for the most accurate results. The most common occurrence of the difficulty lies in some of the sharp angles at wire junctions, where wires may penetrate the adjacent segment center region and create current calculation errors without triggering a warning.

In all cases, the serious modeler must keep an eye on the average gain test (AGT) score to hold it as close as feasible to the ideal value of 1.000. Since our goal is a comparison of general properties and not an exercise that will result in a prototype, we may use values between 0.995 and 1.005 as acceptable AGT scores.

The Single-Bay LPDA "Standard"

Isbell and Carrel's work on the LPDA in the very early 1960s became encoded in many forms, and the design procedures applicable to LPDAs appear in many sources. One often-used progression appears in Chapter 1 of *LPDA Notes* and in Chapter 10 of *The ARRL Antenna Book*, following the Rhodes' *QST* article of November, 1973 ("The Log-Periodic Dipole Array," pp. 16-22). An additional version appeared in "Log-Periodic Antenna Design," *Ham Radio*, December, 1979, pp. 34-39. Examples of further design procedures appear in Lo and Lee, *Antenna Handbook* (1993), Vol. 2, pp. 9-28, and in Balanis, *Antenna Theory: Analysis and Design*, 2nd Ed. (1997), pp. 561-563. There are computer programs devoted to LPDA design, such as LPCAD 3.2, by Roger Cox, WB0DGF. We need not here track the progression of small corrections that have improved the procedures over the years. The design that we shall use as our sample derives simply from the dimensions in **Fig. 5**.

We may model a 20-element planar LPDA using a τ of 0.9 and a σ of 0.167 to arrive at an array with a total angle across the virtual outline of the elements of about 17°. Although this array has half the total elements of the 2-bay models that we shall explore in zig-zag models, basic log-periodic theory takes it to be the equivalent of these arrays that require an optimized value of ψ. Like the other models, our LPDA will use lossless 0.1"-diameter wire throughout in order to equalize any comparisons. In ideal LPDA designs, the element diameter should have a constant length-to-diameter ratio, which would therefore vary the element diameter by the value of τ. In addition, practical versions of the array would use elements having a larger diameter (usually aluminum tubing). The model also uses a 254-Ω phase-line to obtain a feedpoint impedance centered on 200-Ω. A combination of larger elements, τ-tapered elements, and a lower phase-line impedance might yield up to 1 dB additional gain over the version of the array used in this exercise.

Fig. 7 shows the general outline of the LPDA, along with current magnitude distribution graphs for 50, 125, and 200 MHz. The significant current magnitude on the rear elements at 50 MHz suggests that the array might benefit from a slightly longer rear element. As well, the 200-MHz current graphic fails to show a second peak, suggesting that a few more forward elements

might also be useful to overall performance. The LPDA shows peak current on the element (or elements) closest to self-resonance at the operating frequency.

Fig. 7

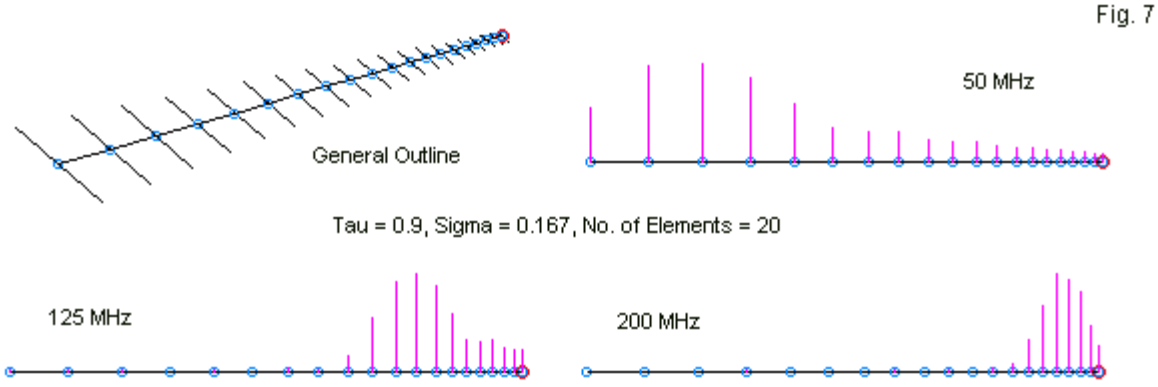

General Outline and Current Magnitude Distribution Along an LPDA
at 3 Frequencies within the Operating Range

In **Fig. 8** we have a different perspective on the relative current magnitude distribution among the LPDA elements. Because each element has two open or free ends, the current distribution on each is perfectly symmetrical. At the lowest frequency within the operating passband (50 MHz), the current on the forward-most element is about 7% of the peak current on the most active element. No element is wholly inert.

Fig. 8

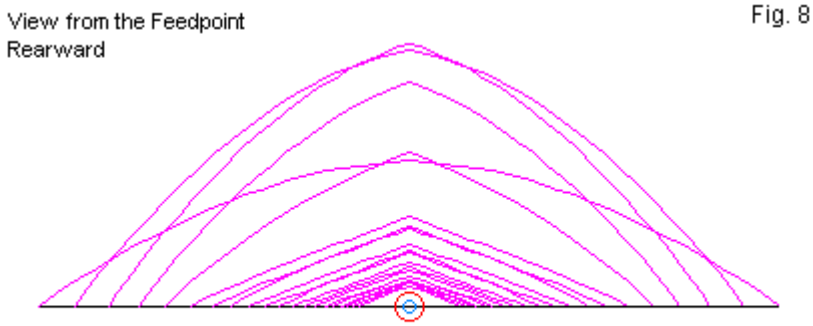

Relative Current Magnitude Distribution on the Elements of
a Single-Bay LPDA at it Lowest Operating Frequency

Table 1 provides sample performance values at 50, 100, 150, and 200 MHz. Since the planar LPDA is not subject to ψ as a variable, both tables are considerably shorter than their zig-zag LPA counterparts. **Fig. 9** follows with a gallery of E-plane and H-plane free-space patterns at the sample frequencies. The performance data and the free-space plots confirm that the LPDA has a slight deficiency in gain and in the front-to-back ratio at the lowest frequency. Therefore, a slightly lower self-resonant frequency for the longest element might well increase the low-end front-to-back ratio and decrease the range of value change—but without significantly changing the average front-to-back value shown in the sweep summary. In addition, one might add one or more dipoles at the forward end, if not to improve gain, then perhaps to enhance pattern control at the upper end of the band. The LPDA shows an increasing beamwidth in the H-plane as we increase the operating frequency, even though the E-plane beamwidth varies by less than 6° across the operating passband.

Table 1. Sample performance values: single-bay LPDA: 20 elements, α' = 17°, τ = 0.9, σ = 0.167

Frequency MHz	Max. Gain dBi	Front-Back Ratio dB	E BW degrees	H BW degrees	Impedance R +/- jX Ω	200-Ω SWR
50	7.33	16.71	67.0	107.8	209 - j 5	1.05
100	8.19	30.77	63.0	94.6	196 - j 30	1.16
150	8.30	29.16	62.6	93.2	180 - j 19	1.16
200	7.88	28.38	63.7	109.4	182 - j 11	1.29

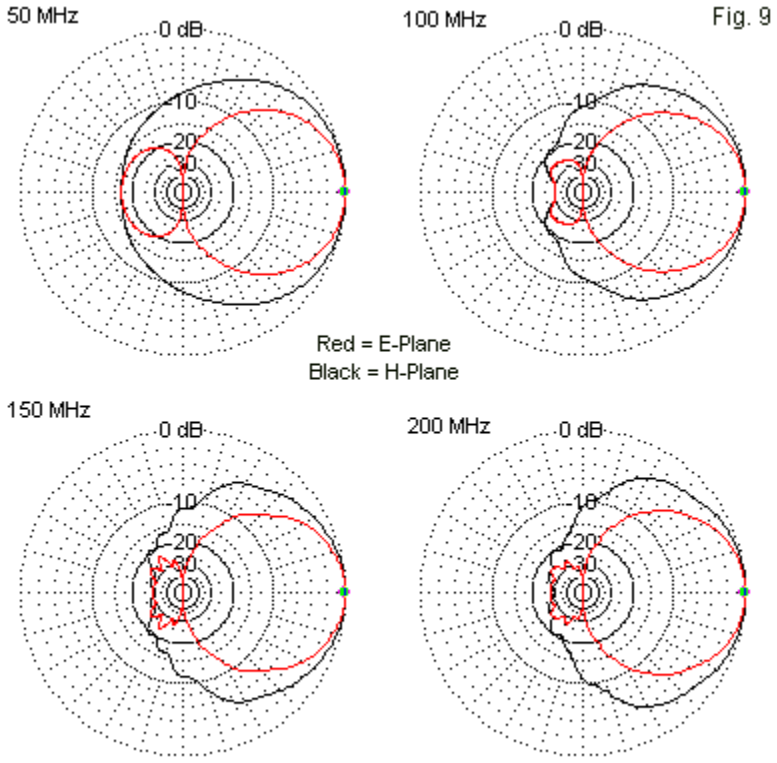

Fig. 9

20-Element LPDA, Alpha' = 17°, Tau = 0.9, Sigma = 0.167
Sample Free-Space E-Plane and H-Plane Patterns

In **Table 2** are the summery values derived from a frequency sweep across the entire operating passband in 5-MHz increments.

Table 2. Sweep data summary, 50-200 MHz in 5-MHz increments: single-bay LPDA: 20 elements, α' = 17°, τ = 0.9, σ = 0.167

Category	Minimum	Maximum	Δ	Average
Gain dBi	7.33	8.52	1.19	8.09
Front-Back dB	16.71	44.56	27.85	28.93
E Beamwidth °	60.8	66.4	5.6	63.7
H Beamwidth °	83.8	109.4	25.6	99.8

Fig. 10 and **Fig. 11** graph the data gathered from the frequency sweeps in terms of forward gain, 180° front-to-back ration, feedpoint resistance and reactance, and the 200-Ω SWR. The

gain and front-to-back graphs shows the decrease in values below about 60 MHz. However, it is useful to note that even with this seeming deficiency, the range of gain variation across the operating passband is less than 1.2 dB. Equally notable is the 200-Ω SWR curve, which never reaches a value of 1.3:1 across the band.

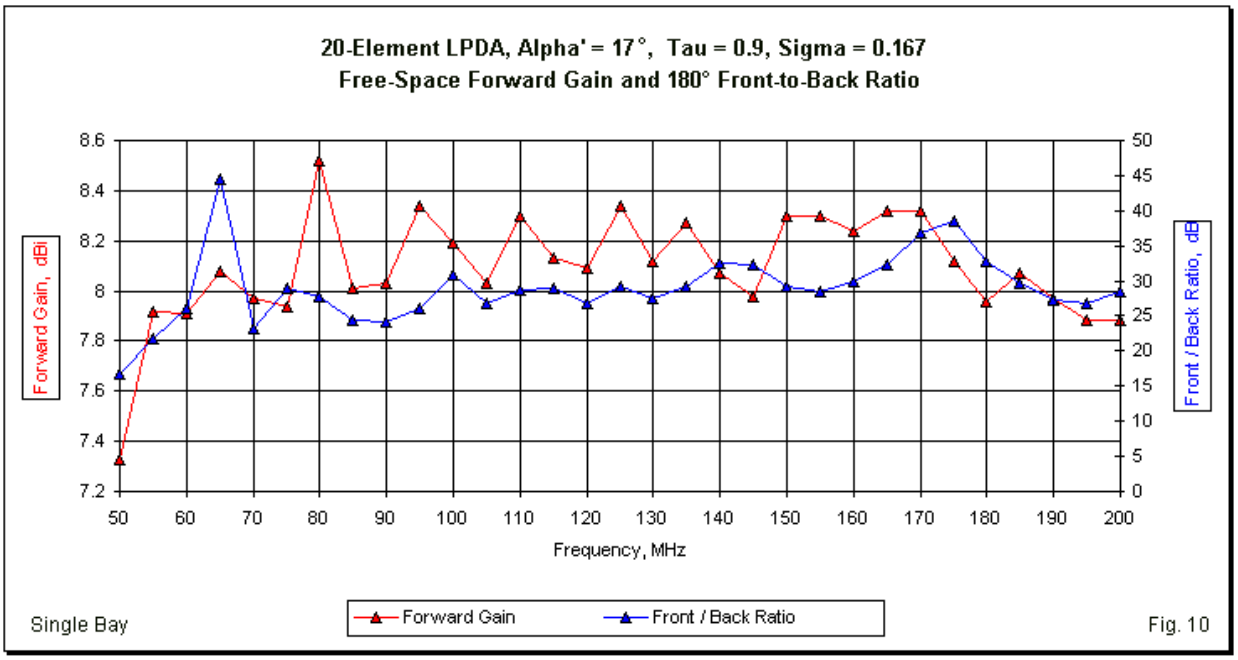

Fig. 10

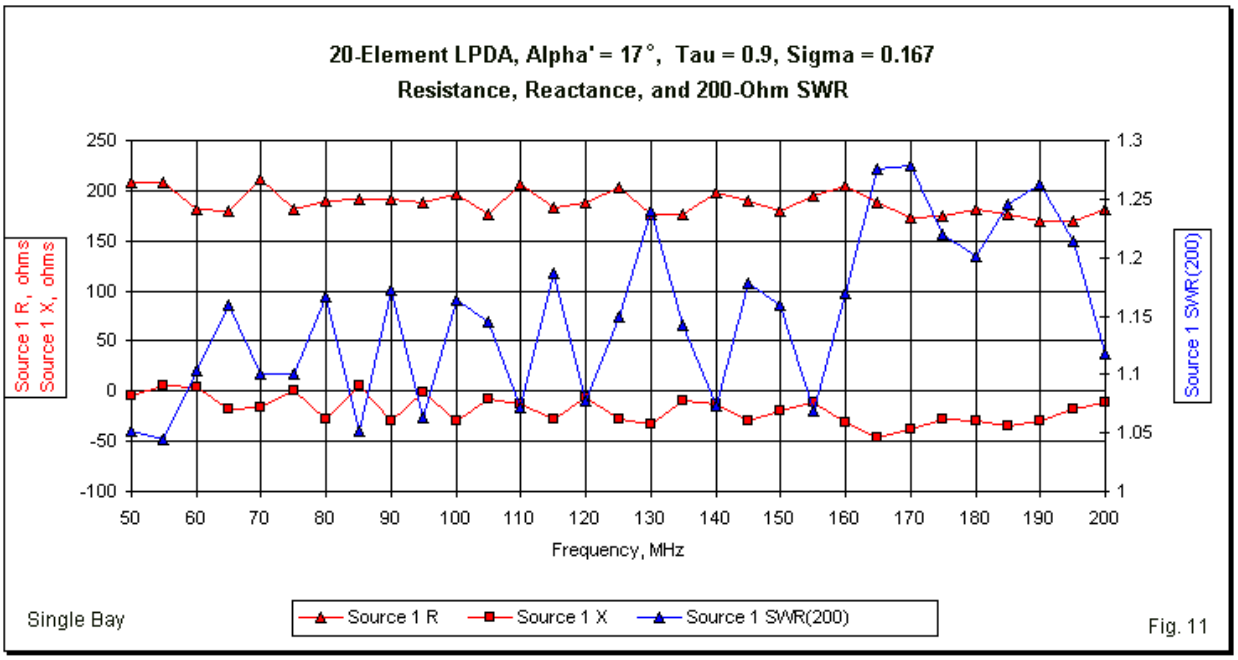

Fig. 11

The LPDA is a single-bay array. Therefore, like any directional antenna composed of dipole elements, the H-plane beamwidth is naturally wider than the E-plane beamwidth. The average beamwidth values are similar to those that we associate with a long-boom (>0.32 λ) 3-element Yagi (normally using larger-diameter elements), and the average LPDA forward gain is slightly

higher when we consider the element diameter used in the model (0.1”). (In comparison, a 3-element Yagi with a short boom of less than 0.23 λ would show about a dB less gain and somewhat larger beamwidth values.)

2-Bay LPDAs

Although I know of only a few commercial examples of wire LPDAs that use two bays, we should examine the possibility to form one more comparator with the zig-zag LPAs that must use two bays. Unlike early zig-zag LPAs that combined low values of τ with high values of ψ, a successful 2-bay LPDA stack requires much narrower angles. In addition, the two LPDA bays must be fed in phase. Nevertheless, the use of a constant angle between the bays provides a constant distance between them as measured in wavelengths for any operating frequency. To sample the performance trends for such arrangements, I created 2-bay models using ψ-angles of 5°, 10°, and 15°. **Fig. 12** shows the general outline of the models with side views of each array angle.

Fig. 12

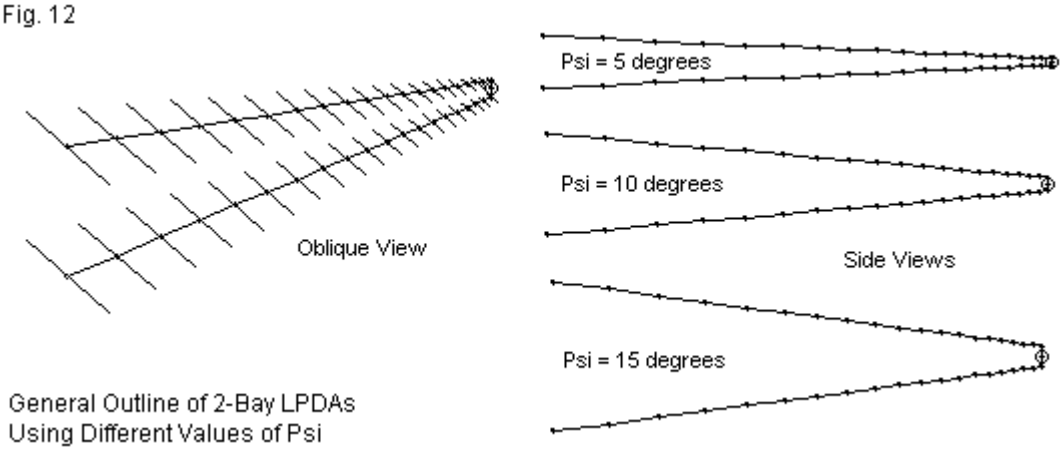

General Outline of 2-Bay LPDAs
Using Different Values of Psi

For comparison with the single-bay data in **Table 1**, I extracted free-space information on each model at 50, 100, 150, and 200 MHz. The additional data appear in **Table 3**. Compared to the single-bay version, the parallel feed for the 20bay models yields a reference impedance of 100 Ω for tabulating SWR values. Although a small matter, the highest SWR value is less than 1.2:1, compared to the single-bay maximum value of nearly 1.3:1. At any of the sampled values of ψ, the 2-bay LPDA is a very stable array with respect to the source impedance.

Table 3. Sample performance values: 2-bay LPDAs: 20 elements, α’ = 17°, τ = 0.9, σ = 0.167

Ψ = 5°

Frequency MHz	Max. Gain dBi	Front-Back Ratio dB	E BW degrees	H BW degrees	Impedance R +/- jX Ω	200-Ω SWR
50	9.09	18.10	61.4	83.2	94 - j 7	1.10
100	9.82	39.75	57.0	74.4	94 - j 9	1.12
150	9.88	47.35	57.0	74.2	97 - j 11	1.12
200	9.55	39.30	57.5	75.2	100 - j 11	1.11

Ψ = 10°

Frequency MHz	Max. Gain dBi	Front-Back Ratio dB	E BW degrees	H BW degrees	Impedance R +/- jX Ω	200-Ω SWR
50	9.35	14.28	61.0	73.2	89 - j 2	1.13
100	10.17	36.27	57.8	68.4	93 - j 8	1.11
150	10.31	42.41	57.4	66.4	98 - j 12	1.14
200	9.85	48.23	57.8	69.2	99 - j 12	1.13

Ψ = 15°

Frequency MHz	Max. Gain dBi	Front-Back Ratio dB	E BW degrees	H BW degrees	Impedance R +/- jX Ω	200-Ω SWR
50	9.70	11.19	61.6	61.7	88 + j 9	1.18
100	10.40	26.23	57.2	59.0	96 - j 2	1.04
150	10.20	29.51	60.6	62.0	101 - j 17	1.19
200	10.34	33.26	61.0	60.0	96 - j 17	1.19

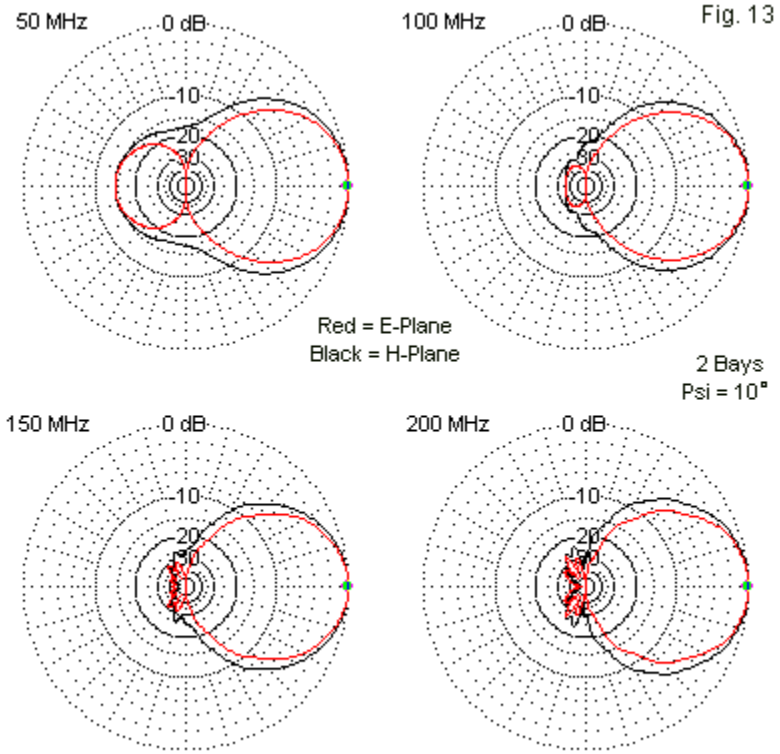

Fig. 13

20-Element LPDA, Alpha' = 17°, Tau = 0.9, Sigma = 0.167
Sample Free-Space E-Plane and H-Plane Patterns

To go with the data on the E-plane and H-plane beamwidths, **Fig. 13** presents combined free-space patterns for the version using a ψ-angle of 10°. As we increase the value of ψ, the H-plane beamwidth decreases with almost no effect upon the E-plane beamwidth. At an angle of 15°, the two beamwidth values are virtually equal.

Selecting the 2-bay model with ψ=10° as the graphic representative of all three 2-bay models emerges most clearly if we tabulate some of the summary data from frequency sweeps made for all of the models. **Table 4** presents information that we may directly compare with the information in **Table 2** for the single-bay LPDA.

Table 4. Sweep data summary, 50-200 MHz in 5-MHz increments: 2-bay LPDAs: 20 elements, α' = 17°, τ = 0.9, σ = 0.167

Ψ=5°

Category	Minimum	Maximum	Δ	Average
Gain dBi	9.09	10.00	0.91	9.72
Front-Back dB	18.10	54.74	36.64	36.02
E Beamwidth °	55.4	61.4	6.0	57.6

Ψ=10°

Category	Minimum	Maximum	Δ	Average
Gain dBi	9.35	10.79	1.18	10.00
Front-Back dB	14.28	63.75	49.47	35.93
E Beamwidth °	54.0	61.0	7.0	57.8

Ψ=15°

Category	Minimum	Maximum	Δ	Average
Gain dBi	9.70	10.79	1.09	10.39
Front-Back dB	11.19	42.10	30.91	28.27
E Beamwidth °	54.4	62.8	8.4	58.8

Early on, investigators recognized that as we increase the ψ-angle of an LPA, the gain increases while the front-to-back ratio decreases. Ordinarily, the front-to-back ratio becomes too small for effective directional array use before the gain ceases to rise. Those trends also apply to 2-bay LPDAs, as the table indicates. The phenomenon shows up most clearly at the lowest operating frequency, where gain is minimum due to the inadequate length of the rear element in the model. However, the same situation also appears in the columns for maximum and average values.

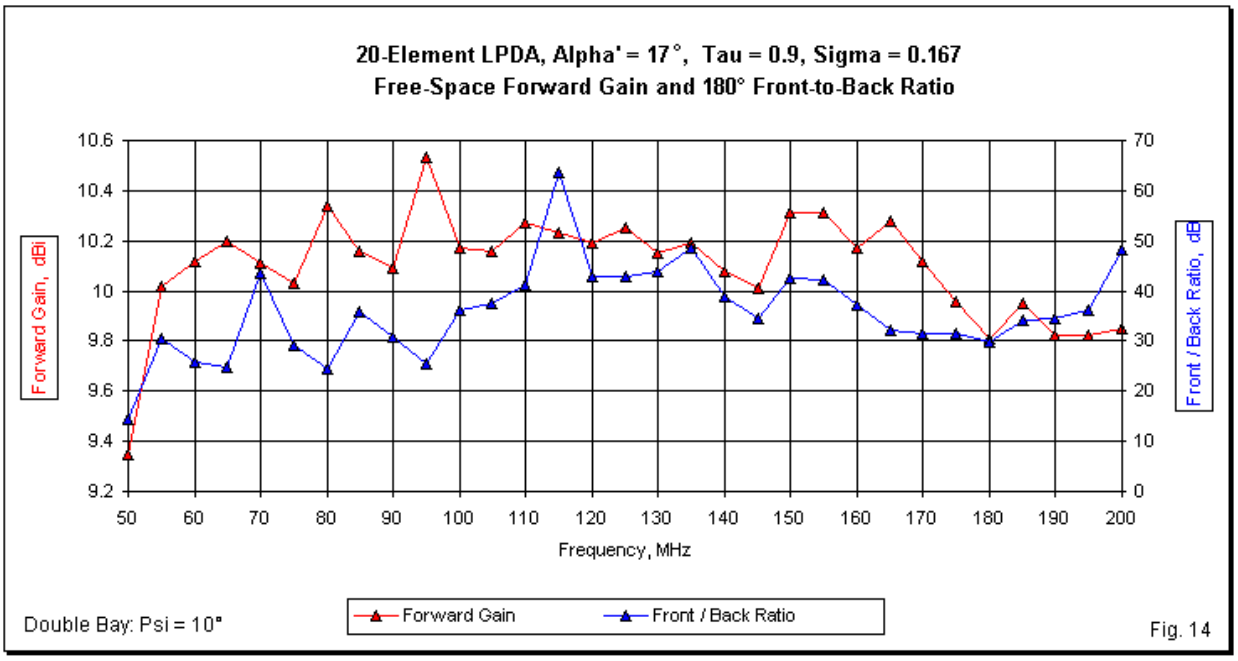

Fig. 14

Fig. 14 provides sweep graphs of free-space forward gain and the 180° front-to-back ratio of the models using a ψ-angle of 10°. The performance weakness below 55 MHz shows itself very clearly. Note also the smaller but evident decrease in gain performance at the high end of the passband. 2-bay LPDAs tend to reflect whatever large or small weaknesses that we design into the root single-bay version of the antenna. The front-to-back data, however, requires some caution. Although the values are very high, compare the sample E-plane patterns in **Fig. 13** with the corresponding single-bay patterns in **Fig. 9**. The 180° value of the front-to-back ratio is not always a sufficient indicator of rearward performance. Examining the strongest rearward lobes is always good practice in evaluating array performance.

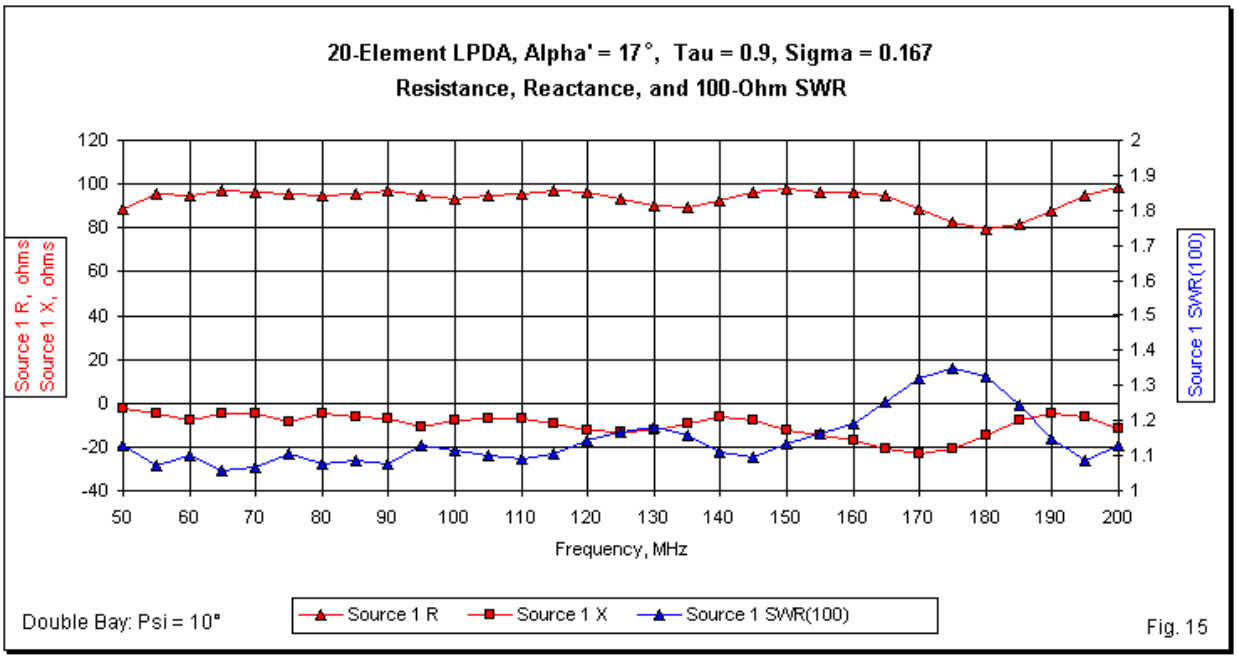

Fig. 15 provides a graph of the feedpoint performance in terms of the source resistance and reactance, as well as the 100-Ω SWR across the operating passband. Because the SWR values use a different Y-axis maximum value relative to the values shown for the single-bay model in **Fig. 11**, we may legitimately wonder if the smoothness of the curves in the present graph is real or illusory. A comparison between the resistance and reactance curves in the two graphs will establish that the double-bay array shows smoother impedance performance across the operating range.

Table 5. LPDA sweep data summary, 50-200 MHz in 5-MHz increments: 20 elements, α' = 17°, τ = 0.9, σ = 0.167

Single-bay Category	Minimum	Maximum	Δ	Average
Gain dBi	7.33	8.52	1.19	8.09
Front-Back dB	16.71	44.56	27.85	28.93
E Beamwidth °	60.8	66.4	5.6	63.7
H Beamwidth °	83.8	109.4	25.6	99.8

Double-bay, Ψ=10°

Category	Minimum	Maximum	Δ	Average
Gain dBi	9.35	10.79	1.18	10.00
Front-Back dB	14.28	63.75	49.47	35.93
E Beamwidth °	54.0	61.0	7.0	57.8

To determine whether the 2-bay LPDA provides a significant advantage over its single-bay root antenna, let's compare the summary sweep data for each, using the ψ=10° version of the larger array. **Table 5** allows some ready conclusions. For example, even though the arrays are not optimally spaced relative to our experience with narrow-band antennas such as Yagi-Uda arrays, we obtain a consistent 2-dB gain advantage from the double-bay LPDA. Although the front-to-back ratio for the 2-bay antenna appears to be higher, the advantage may be illusory, since the values at the lowest operating frequency show a reverse trend. Except for the lowest operating frequencies, the front-to-back ratios of both versions of the LPDA are well above 20 dB, largely making comparisons academic.

One advantage of the 2-bay LPDA cannot be shown with free-space models. A single-bay LPDA will normally be installed over ground at a constant physical height. For HF versions of such arrays, the take-off angle will vary with the frequency of operation. We may angle a 2-bay array in such a manner that the take-off angle is virtually constant across a wide frequency range. TCI has long marketed an LPA with just such properties.

It is obvious that the text of these initial notes cannot contain all of the data gathered on all of the LPDA models. Therefore, I have gathered the data collection for the LPDAs and the zig-zag LPAs into a special appendix for leisurely viewing.

Conclusion to Part 1

In these initial notes, we have surveyed—perhaps too rapidly—some of the background and design considerations that go into LPAs of all sorts. In addition, we have set up the now-standard LPDA version of the antenna as a standard against which we may compare the performance of both trapezoidal and X (saw tooth) LPAs in the next two parts of our sojourn in the land of linear-element log-periodic arrays. Although 2-bay LPDAs are rare, I have included models for them, since all of the ensuing zig-zag arrays must use a 2-bay structure to obtain significant directional gain.

Where these notes differ most radically from older practice lies in the basic design parameters. I have selected values of τ, σ, and α (or α') that are optimally related. The choice of τ=0.9 produces reliable good results with no anomalous frequencies in the sweep range, even though it does not yield the maximum gain obtainable from an LPDA. Rather, it achieves good performance while allowing NEC-4 models having a manageable size. Likewise, the element diameter (0.1") allows the models to avoid pressing any NEC-4 limitations, even though fatter elements may produce higher gain values.

Values of ψ emerge from experimental modeling exercises, and the ultimate selection of a ψ-angle may rest on performance objectives and construction limitations that fall outside the scope of this exercise. My selection of a representative example for 2-bay LPAs will rest on the simple appearance of best overall performance or other equally quasi-arbitrary criteria. However, the data appendix will provide identical data for all models within the survey. Perhaps the only partially emergent conclusion that we can draw so far regarding the optimal ψ-angle is that as we increase the value of τ and reduce the value of α, the optimal value of ψ will also

decrease. The sampled ψ-angles for 2-bay LPDAs are significantly smaller than those we encounter in older designs for trapezoidal and X LPAs.

In Part 2, we shall examine trapezoidal LPAs, both with and without booms. We may compare the performance of the two zig-zag types and also compare both with LPDA performance, since we shall use the same set of design parameters. As a bonus, we shall examine a trapezoidal zig-zag array of older design.

A Tale of Three LPAs: Some Notes on Zig-Zag Log-Periodic Arrays
2. The Trapezoidal Zig-Zag LPA

L. B. Cebik, W4RNL

Among the earliest 2-bay directional LPA designs was the trapezoidal zig-zag array. By 1960, Collins was producing a number of LPAs under the "327" designation, and an 11-60-MHz trapezoidal array with self-supporting tubular elements proved to be perhaps the most photogenic. The trapezoidal design also proved suitable for television reception with a design range of 48 to 230 MHz. In fact, the operating range (50-200 MHz) that we use in our modeling comparisons derives from the television LPDA, which radio amateurs adapted to use on 6, 4, 2, and 1.25 meter bands, depending upon one's location.

In this part of our exploration of the zig-zag LPA, we shall examine trapezoidal LPAs, beginning with those that employ a boom. **Fig. 1** shows the outline of a single trapezoidal bay, a 2-bay version, and side views of a range of versions showing different ψ-angles. All of the model outlines that appear in the figure employ a boom, the preferred configuration for the trapezoidal LPA. However, boomless versions are also theoretically possible, so we shall examine them also. Before we conclude this part, we shall also look at an older design from amateur literature, one that uses quite different values for α, τ, and ψ than we are employing in our attempt at a fair comparison among LPA varieties.

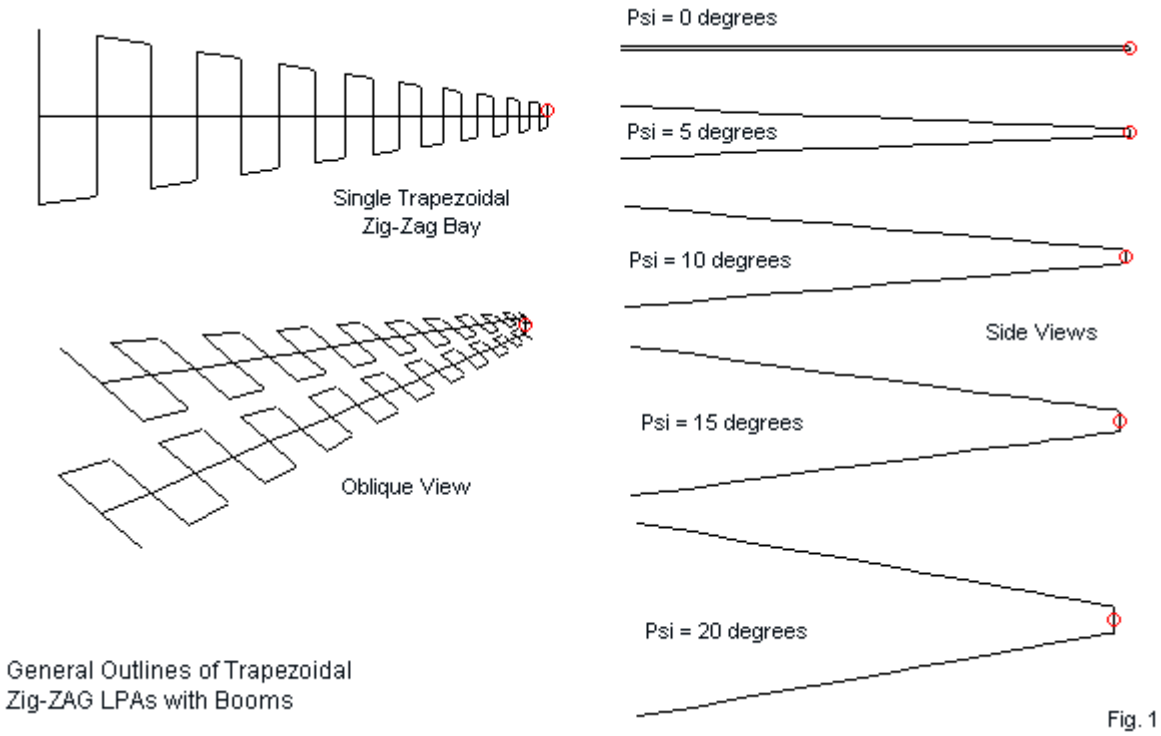

Fig. 1

Early zig-zag LPAs generally used quite large values for α, mostly for the practically reason of arriving at relatively short array boom lengths. 60° was perhaps the most common angle to appear in literature and commercial designs. Arrays also used τ-values between 0.6 and 0.8 to reduce the element count and arrive at a lighter overall structure. (Most LPDA literature recommends no τ-value below about 0.8, with higher values necessary to reduce the potential

for the appearance of anomalous frequencies.) The most common ψ-angles seem to have been 35° to 45°.

Our comparison designs all use the following values: α' = 17°, τ = 0.9, σ = 0.167, the optimum value for the selected value for τ. Therefore, the trapezoidal LPAs that we explore for most of our work in this part will use the dimensions shown in **Fig. 2**. The trapezoidal element lengths—counting only from side-to-side—will be identical to those used in Part 1's LPDA. As well, the models will use 20 elements per bay. All models will be in free space and use 0.1" (2.54-mm) lossless wire for reasons outlined in Part 1.

Zig-Zag Log-Periodic Antenna Elements											Fig. 2
Work Sheet		**Bold = User Entry**									
Tau		**0.90**								Sigma	0.167
Alpha'	degrees	**17.00**	degrees	0.297	radians	1/2Alpha'	0.148	tanAlpha	0.1495		0.167
F-low		**50.00**	MHz								
F-high		**200.00**	MHz								
L-long		3.00	meters	9.84	feet	118.11	inches				
Lhigh		0.75	meters	2.46	feet	29.53	inches				
L*1.6		0.47	meters	1.54	feet	18.45	inches				
Rv	Vertex R	10.04	meters	32.93	feet	395.15	inches				
Element	Ln	Ln/2	Rn	Element	Lfeet	Lft/2	Rfeet	Element	Linch	Lin/2	Rinch
1	3.00	1.50	10.04	*1*	9.84	4.92	32.93	*1*	118.11	59.06	395.15
2	2.70	1.35	9.03	*2*	8.86	4.43	29.64	*2*	106.30	53.15	355.63
3	2.43	1.22	8.13	*3*	7.97	3.99	26.67	*3*	95.67	47.83	320.07
4	2.19	1.09	7.32	*4*	7.18	3.59	24.01	*4*	86.10	43.05	288.06
5	1.97	0.98	6.59	*5*	6.46	3.23	21.60	*5*	77.49	38.75	259.26
6	1.77	0.89	5.93	*6*	5.81	2.91	19.44	*6*	69.74	34.87	233.33
7	1.59	0.80	5.33	*7*	5.23	2.62	17.50	*7*	62.77	31.38	210.00
8	1.43	0.72	4.80	*8*	4.71	2.35	15.75	*8*	56.49	28.25	189.00
9	1.29	0.65	4.32	*9*	4.24	2.12	14.17	*9*	50.84	25.42	170.10
10	1.16	0.58	3.89	*10*	3.81	1.91	12.76	*10*	45.76	22.88	153.09
11	1.05	0.52	3.50	*11*	3.43	1.72	11.48	*11*	41.18	20.59	137.78
12	0.94	0.47	3.15	*12*	3.09	1.54	10.33	*12*	37.06	18.53	124.00
13	0.85	0.42	2.83	*13*	2.78	1.39	9.30	*13*	33.36	16.68	111.60
14	0.76	0.38	2.55	*14*	2.50	1.25	8.37	*14*	30.02	15.01	100.44
15	0.69	0.34	2.30	*15*	2.25	1.13	7.53	*15*	27.02	13.51	90.40
16	0.62	0.31	2.07	*16*	2.03	1.01	6.78	*16*	24.32	12.16	81.36
17	0.56	0.28	1.86	*17*	1.82	0.91	6.10	*17*	21.89	10.94	73.22
18	0.50	0.25	1.67	*18*	1.64	0.82	5.49	*18*	19.70	9.85	65.90
19	0.45	0.23	1.51	*19*	1.48	0.74	4.94	*19*	17.73	8.86	59.31
20	0.41	0.20	1.36	*20*	1.33	0.66	4.45	*20*	15.95	7.98	53.38

NEC-4 models of the trapezoidal zig-zag LPA are necessarily larger than comparable LPDA 2-bay models, with some models exceeding 1600 segments. Trapezoids require wires for both the boom (where used) and the wires that connect alternating element ends. The goal, within the limits of the segmentation process is to have all segments be the same length throughout the model. In addition, the segment length should also be within NEC limits at both the upper and the lower end of the operating range.

A number of published designs show the most forward element end and the boom brought to the vertex as a feedpoint location. However, considerable experimentation with variations showed no significant difference in performance in any category between this complex system and the simpler version used in the models. Models with booms add a wire that connects the two booms at the short end of the array and places the model source at the center of this wire. Models without booms add a wire connecting the free ends of the most forward element in each bay, with the source at its center.

Trapezoidal LPAs with Booms

Trapezoidal LPAs with booms derive most clearly from early versions of log-periodic structures using solid elements instead of the wire outline of those elements. We can easily picture these bays by using **Fig. 1** and simply filling in the area created by each closed trapezoidal structure. Experimental designs also tended to use a boom that became wider as the elements became longer, but practicalities reduced the boom to a constant diameter. In commercial and amateur versions of the antenna, the boom often used a larger diameter than the elements to provide structural support.

Trapezoids with booms show the general ability of a wire-outline version of the LPA to mimic the behavior of their solid surface counterparts. **Fig. 3** shows the 50-MHz current magnitude distribution along the wires of an array. The lower section of the graphic reveals the parallel current magnitude curves for each closed trapezoidal structure—at least for the longest elements that allow visual resolution of the curves.

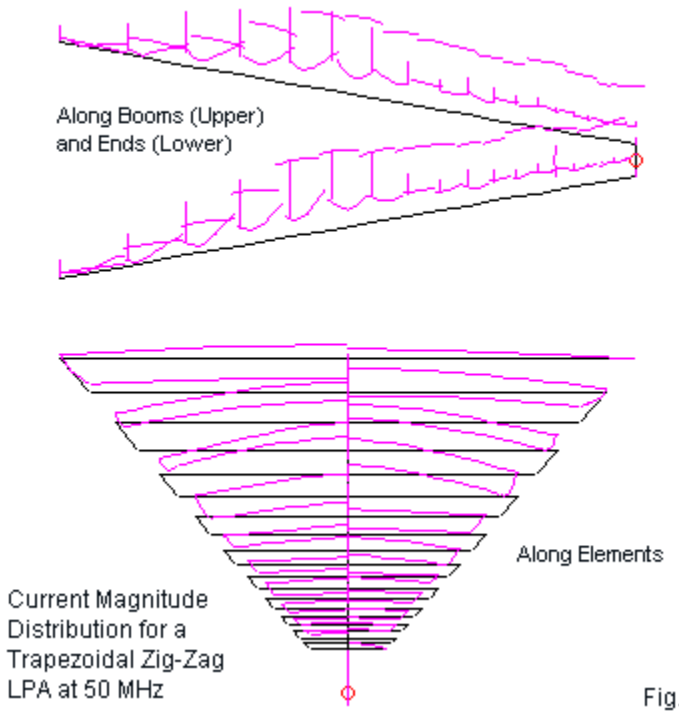

Fig. 3

The upper portion of the figure is equally significant, but for a different reason. The LPDAs shown in Part 1 presented the highest current magnitudes on the elements of the array closest to self-resonance at the operating frequency. Hence, the highest current at 50 MHz occurred on the second or third element from the rear of the array. In **Fig. 3**, the vertical lines represent peak relative element current, while the horizontal lines portray the current along the booms (upper lines) and the wire ends that close trapezoids (lower lines). Allowing for the sloping base lines of each bay, the peak current at the lowest operating frequency occurs well forward of the elements that are closest to self resonance. A similar situation will appear in boomless versions of the zig-zag trapezoidal LPA and in X versions of the antenna.

2-bay LPAs, with each bay transposing the closed trapezoids, are necessary to produce directional properties. It is tempting to think of the booms as constituting a phase line comparable to the line used to connect the dipoles of an LPDA. However, whenever we create a ψ-angle of any significant proportions, the spacing between the booms is too great for the structure to exhibit transmission-line properties. Indeed, the elements in each bay, with alternating directions, are capable of showing relatively correct relationships to each other at any given point along the length of the LPA, even without a boom. As we shall see, however, the presence of the boom enhances performance considerably by replicating in a wire-outline LPA the properties of the solid-surface LPA designs from which it derives.

One reason for including a version of the array using a ψ-angle of 0° is to allow us to see the change in the reference feedpoint impedance as the ψ-angle increases and as any transmission-line properties between booms disappear. We can see this and other changes by surveying sample performance properties of the five versions of the array at 50, 100, 150, and 200 MHz. **Table 1** provides the results in tabular form. Note initially the change in the reference impedance for the reported SWR values between ψ-angles of 5° and 10°.

Table 1. Sample performance values of trapezoidal zig-zag LPAs using various ψ-angles

1. 20 elements/bay, α = 17°, τ = 0.9, ψ = 0° (flat array, 4" separation between bays)

Frequency MHz	Max. Gain dBi	Front-Back Ratio dB	E BW degrees	H BW degrees	Impedance R +/- jX Ω	225-Ω SWR
50	7.17	27.83	70.6	113.8	240 - j 9	1.08
100	7.58	28.60	68.8	106.5	242 - j 2	1.08
150	7.61	24.91	67.8	107.4	222 - j 13	1.06
200	7.24	20.60	71.4	111.4	149 + j 28	1.55

2. 20 elements/bay, α = 17°, τ = 0.9, ψ = 5°

Frequency MHz	Max. Gain dBi	Front-Back Ratio dB	E BW degrees	H BW degrees	Impedance R +/- jX Ω	225-Ω SWR
50	8.34	30.50	65.1	94.4	261 - j 13	1.17
100	8.43	29.21	65.2	94.2	239 - j 6	1.07
150	8.20	25.16	65.4	97.4	225 - j 0	1.00
200	7.71	20.13	68.8	103.4	149 + j 39	1.59

3. 20 elements/bay, α = 17°, τ = 0.9, ψ = 10°

Frequency MHz	Max. Gain dBi	Front-Back Ratio dB	E BW degrees	H BW degrees	Impedance R +/- jX Ω	300-Ω SWR
50	9.16	26.94	64.0	82.8	293 + j 8	1.04
100	9.20	24.47	64.4	82.9	272 + j 33	1.17
150	8.90	20.91	65.0	85.6	259 + j 86	1.41
200	8.33	16.04	68.2	88.8	178 + j159	2.32

4. 20 elements/bay, α = 17°, τ = 0.9, ψ = 15°

Frequency MHz	Max. Gain dBi	Front-Back Ratio dB	E BW degrees	H BW degrees	Impedance R +/- jX Ω	300-Ω SWR
50	9.63	22.63	64.8	71.2	321 + j 17	1.09
100	9.51	21.90	65.3	72.4	314 + j 78	1.29
150	9.19	18.57	66.6	73.6	306 + j173	1.76
200	8.52	13.71	69.0	74.4	241 + j307	3.02

5. 20 elements/bay, α = 17°, τ = 0.9, ψ = 20°

Frequency MHz	Max. Gain dBi	Front-Back Ratio dB	E BW degrees	H BW degrees	Impedance R +/- jX Ω	300-Ω SWR
50	9.86	16.26	67.2	60.8	326 + j 10	1.09
100	9.68	18.87	67.1	61.1	351 + j 96	1.40
150	9.16	17.00	72.4	61.8	348 + j244	2.12
200	8.59	12.56	72.0	62.4	345 + j460	3.80

The gain figures are especially interesting, since the only difference among the arrays is the ψ-angle. At the lowest values of ψ, the gain at 50 MHz is significantly lower than the gain at 100 MHz. However, in the move between ψ=10° and ψ=15°, the 50-MHz gain rises to exceed the gain at 100 MHz. For all values of ψ, the gain at 200 MHz drops relative to the gain at the two middle frequencies in the sample. The decrease suggests that the design would benefit from additional shorter elements at the forward end of the array—assuming that equal gain across the operating passband is a desirable feature.

These characteristics are reflected in the impedance and SWR performance values. As we increase the ψ-angle, the higher frequencies show increased reactance as measured against the resistive component of the feedpoint impedance. The increasing reactive component also shows up as ever-worsening high-end SWR values relative to the indicated reference impedance.

Like all LPAs, increasing the ψ-angle produces increasing forward gain and decreasing front-to-back ratio values.

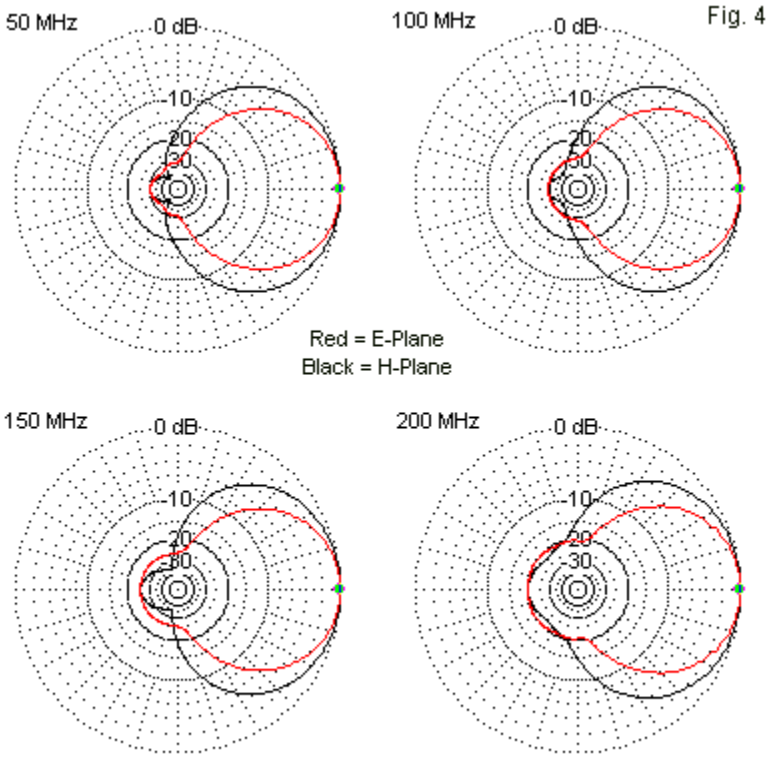

Fig. 4

20 Elements/Bay, Alpha = 17°, Tau = 0.9, Psi = 5°
Sample Free-Space E-Plane and H-plane Patterns

Deciding upon a representative version of the array to provide graphical samples of performance is not easy for trapezoidal LPAs that have booms. Smaller values of ψ show better impedance and front-to-back behavior, while larger ψ-angle values show higher gain. In many ways, the 5° ψ-angle is a compromise. Still, as revealed in **Fig. 4**, the sample patterns for the selected version of the array show excellent pattern control at all frequencies. The H-plane pattern has a wider beamwidth than the E-plane pattern at this ψ angle. In fact, the E-plane and H-plane values to not merge until the ψ-angle reaches about 20°. (The data and graphics for all 5 versions of the trapezoidal LPA with a boom appear in the special data appendix to this series.)

The alternative method of data presentation that we used with the single- and double-bay LPDAs is also applicable to our trapezoidal LPAs. **Table 2** provides succinct summaries of some of the key sweep information for all 5 models.

Table 2. Frequency sweep summery of trapezoidal zig-zag LPAs using various ψ-angles from 50 to 200 MHz

1. ψ = 0°

Category	Minimum	Maximum	Δ	Average
Gain dBi	7.11	8.10	0.99	7.60
Front-Back dB	20.60	28.60	8.00	25.70
E Beamwidth °	65.0	71.6	6.6	68.4

2. ψ = 5°

Category	Minimum	Maximum	Δ	Average
Gain dBi	7.71	8.57	0.86*	8.35
Front-Back dB	20.13	32.04	11.91	27.12
E Beamwidth °	63.0	68.8	5.8	65.0

*Least variation across the passband of the group

3. ψ = 10°

Category	Minimum	Maximum	Δ	Average
Gain dBi	8.33	9.29	0.96	9.07
Front-Back dB	16.04	27.52	11.48	22.63
E Beamwidth °	62.7	68.2	5.5*	64.2

*Least variation across the passband of the group

4. ψ = 15°

Category	Minimum	Maximum	Δ	Average
Gain dBi	8.52	9.65	1.13	9.34
Front-Back dB	13.71	24.29	10.58	19.79
E Beamwidth °	63.2	69.0	5.8	65.4

5. ψ = 20°

Category	Minimum	Maximum	Δ	Average
Gain dBi	8.59	9.91	1.32	9.46
Front-Back dB	12.56	19.98	7.42	16.79
E Beamwidth °	63.4	72.4	9.0	67.2

The selected 5° ψ-angle shows at least 20-dB front-to-back ratio everywhere in the operating range. As the sample patterns show, the 180° value is also the worst-case value for

this array. The average front-to-back value for the sweep decreases steadily with an increasing ψ-angle value, while the average gain-value increases. The E-plane beamwidth values remain relatively stable for all versions of the array. Indeed, the notations relating to the least variation in a performance category are not very significant, since the array show relatively even behavior in almost all versions. Except for the rapid decline in gain at the high end of the passband, the sweep graph for both gain and front-to-back ratio in **Fig. 5** for the 5° ψ-angle version reflects smooth performance with only the normal fluctuations created by the periodic structure. (Engineers already knew much of this behavior in the very late 1970s, as soon as method-of-moments analysis became available.)

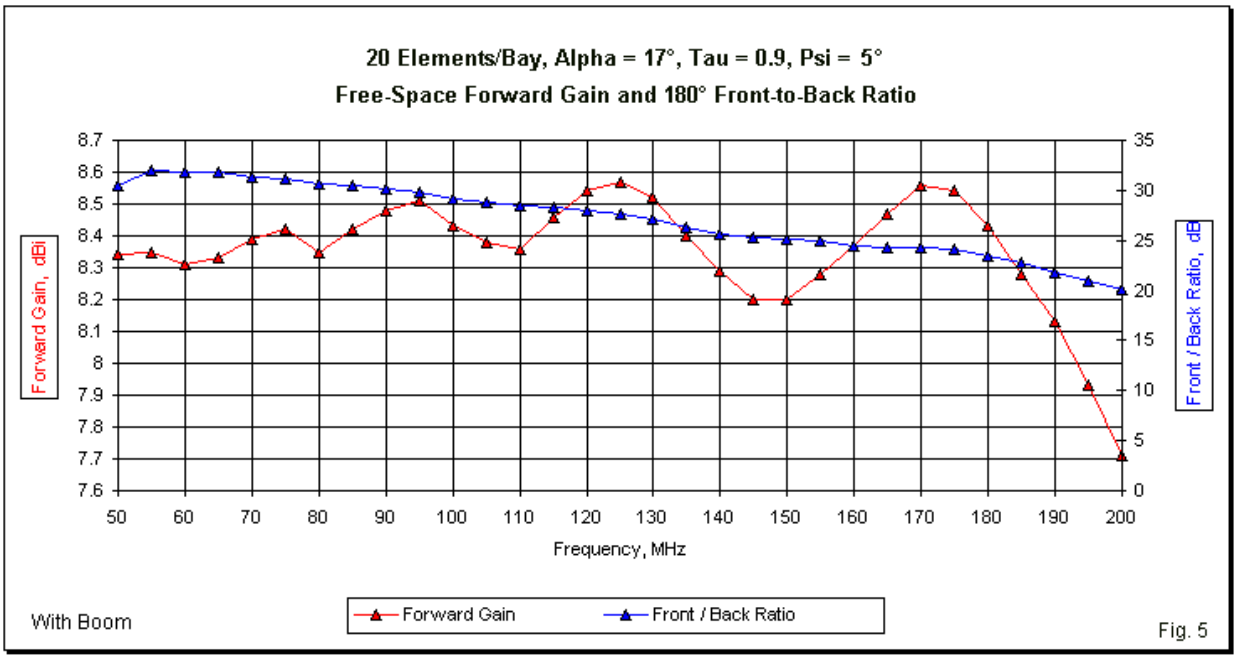

Fig. 5

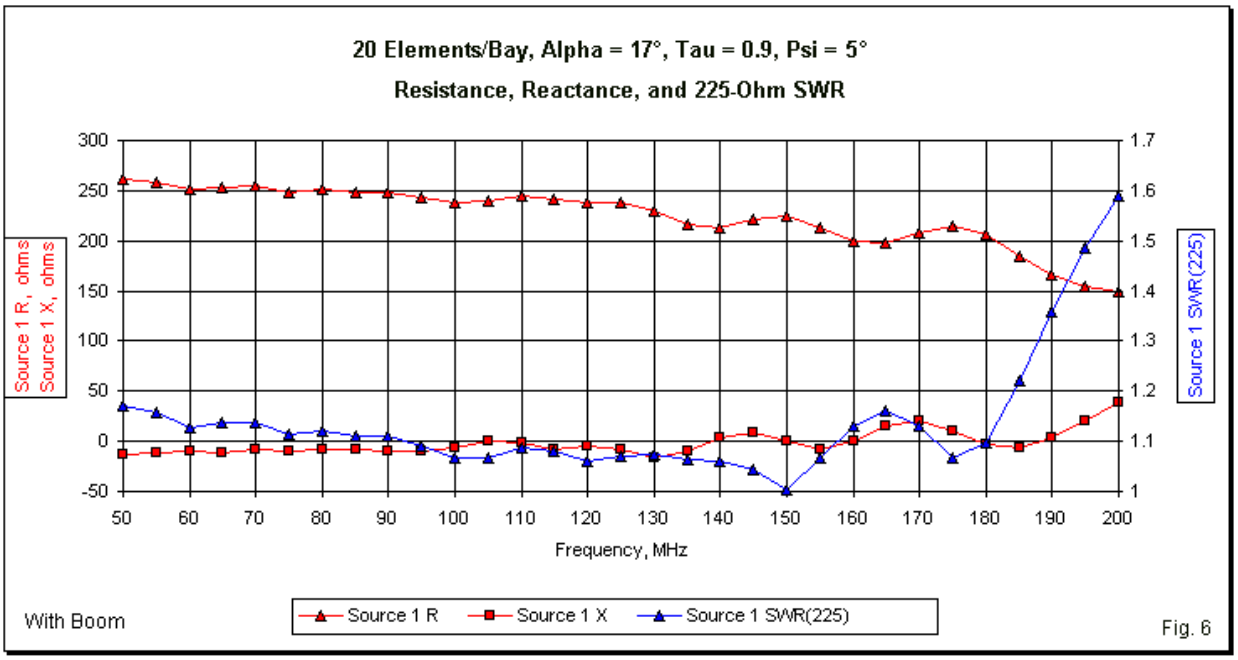

Fig. 6

Fig. 6 provides sweep information on the free-space feedpoint performance in terms of resistance, reactance, and the 225-Ω SWR values. Performance is exceptionally smooth, with only the final 20 MHz of the passband showing the somewhat aberrant rise in the SWR value. As the graph shows, the rising SWR results from a combination of a sinking value for resistance and a slowly rising value of inductive reactance. As we increase the ψ-angle, the impedance curves become sharper with more sudden swings in value and especially a much greater rise in the feedpoint's inductive reactance. See the data appendix for details on the sweeps for all versions of the boom-equipped trapezoidal LPA.

Since the comparisons that we are making lack the imposition of outside construction or applications specifications, I have generally selected the representative example based on the smoothness of performance across the operating passband. External criteria might easily alter the selection for the design. In general, the representative trapezoidal LPA shows performance about mid way between the single- and double-bay LPDAs, although one may alter that position by a judicious selection of the ψ-angle. With a τ of 0.9, an α' of 17°, and a σ of 0.167, the boom-equipped trapezoidal LPA shows a high level of performance. It simplifies construction by not requiring a phase line, but in return, it demands a 3-dimensional structure.

Trapezoidal LPAs without Booms

Although it is theoretically possible to construct boomless trapezoidal LPAs, they are far less common than boomless LPAs using the X configuration. Both types of antenna offer some simplifications of a wire structure. One could build wire or thin-tube UHF versions of the array using a jig composed of a large board and nails to form corners with very small bending radii. **Fig. 7** shows the outline of such an array for 50-200 MHz, which uses the following values: τ = 0.9, α' = 17°, and ψ = 20°. The array uses 20 elements, all 0.1" in diameter, with the longest being a physical half-wavelength at the lowest operating frequency and the longest slightly shorter than a half-wavelength at 1.6 times the highest operating frequency. The dimensions are those in **Fig. 2**.

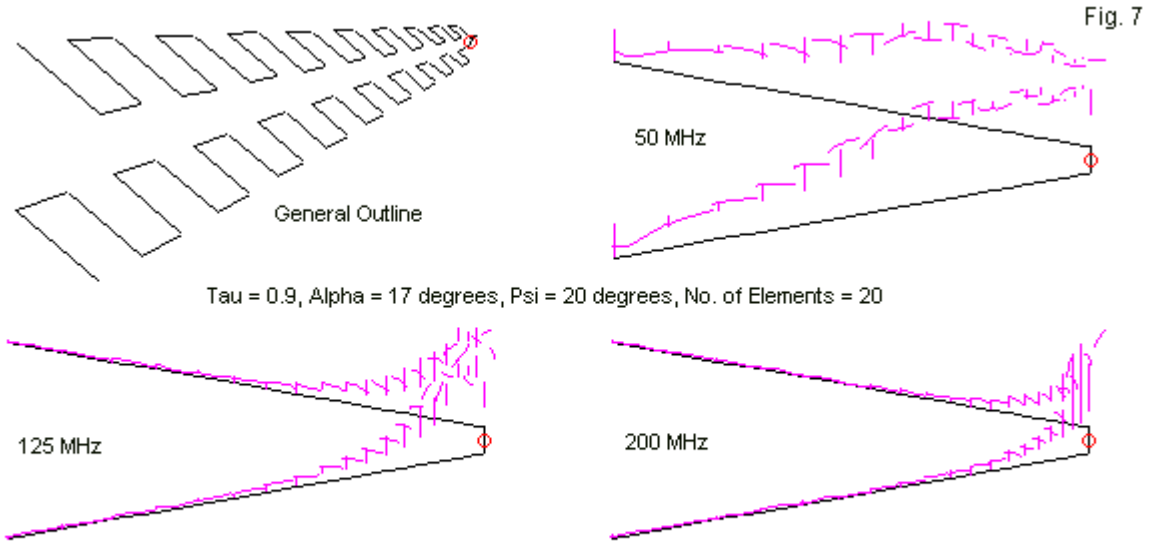

General Outline and Current Magnitude Distribution Along a Trapezoidal Zig-Zag Array at 3 Frequencies within the Operating Range

Obviously, I consider boomless trapezoidal LPAs worth exploration, if only to compare the results with the data collected on trapezoidal zig-zag LPAs with booms. In addition to the outline, the figure contains current magnitude distribution graphs for 50, 125, and 200 MHz. The curves are somewhat difficult to interpret for a trapezoidal zig-zag array because the lines include current on the parallel elements (the vertical lines) and on the element-end linking wires (more horizontal lines). The element currents show the peak value of the current, which may occur anywhere along the element. Perhaps the most interesting fact about the curves is that they do not show maximum values very close to the element that is closest to resonance, as they do in comparable graphs for LPDAs. Instead, the peak current occurs generally much farther forward along the array. In this respect, they share a common general feature with boom-equipped versions of the array.

Fig. 8

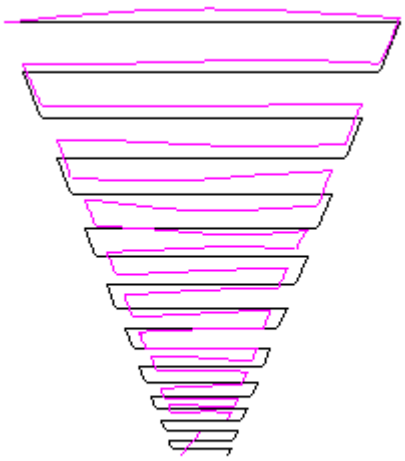

50-MHz Current Magnitude Distribution
Along One Element Bay of a Trapezoidal
Zig-Zag LPA

Part of the reason for the seemingly displaced current maximum that is most apparent at the low end of the operating range results from the absence of the end-effect on the elements. Only the longest element in each bay has a free end. The end-wires have significant current magnitude and play a role in the transitions from one element to the next. As shown in the isolated bay curves in **Fig. 8**, mid-element current magnitude on some of the middle-length element may actually reach a minimum. Unlike the boom-equipped versions of the trapezoidal LPA, the boomless versions show no signs of correspondence to solid-surface LPAs that preceded them.

I modeled 4 versions of the 20-element trapezoidal zig-zag LPA, varying the value of ψ in 5° increments from 10° to 25°. One might experimentally replicate the exercise by using a variable angular brace in the general support structure for each bay. The volume of data collected is too great for inclusion in these notes. Therefore, I have made available a final document to serve as a data appendix for the complete data set. Here, we shall sample the data in two ways. The first is a table of sample performance information for 50, 100, 150, and 200 MHz for each of the 4 versions of the array. See **Table 3**. The most immediately striking fact is that the reference feedpoint impedance for the boomless trapezoids is about twice the value for version that use booms. Besides the difference in the reference impedance, the SWR value progression for each array resembles the progressions for versions with booms for ψ-angles between 10° and 20°. However, the cause of the rise is different. With boom-equipped arrays, the chief source

of higher SWR values was an increase in reactance. With the boomless versions, the chief cause is a rapid rise in the feedpoint resistance.

Table 3. Sample performance values: trapezoidal array: 20 elements/bay, α = 17°, τ = 0.9

1. ψ = 10°

Frequency MHz	Max. Gain dBi	Front-Back Ratio dB	E BW degrees	H BW degrees	Impedance R +/- jX Ω	600-Ω SWR
50	6.20	9.85	101.1	102.4	566 + j 79	1.16
100	6.49	16.31	95.8	104.6	562 + j 99	1.20
150	6.26	16.26	101.6	110.2	521 + j 37	1.17
200	3.05	7.27	182.0	173.8	723 + j595	2.44

2. ψ = 15°

Frequency MHz	Max. Gain dBi	Front-Back Ratio dB	E BW degrees	H BW degrees	Impedance R +/- jX Ω	600-Ω SWR
50	6.34	8.94	107.2	94.6	530 + j 13	1.14
100	6.88	16.55	94.5	90.6	534 + j100	1.24
150	6.56	16.23	99.8	96.8	543 + j 65	1.16
200	3.62	5.95	179.4	129.4	958 + j596	2.43

3. ψ = 20°

Frequency MHz	Max. Gain dBi	Front-Back Ratio dB	E BW degrees	H BW degrees	Impedance R +/- jX Ω	600-Ω SWR
50	6.20	6.97	120.0	86.6	559 + j 1	1.07
100	7.02	10.51	96.2	76.6	550 + j121	1.26
150	6.63	13.57	103.7	86.2	594 + j 87	1.16
200	4.48	4.68	170.0	93.6	1378 + j345	2.47

4. ψ = 25°

Frequency MHz	Max. Gain dBi	Front-Back Ratio dB	E BW degrees	H BW degrees	Impedance R +/- jX Ω	600-Ω SWR
50	5.81	7.58	143.2	84.8	692 - j 57	1.18
100	7.43	6.87	89.2	61.8	590 + j139	1.26
150	6.67	8.20	108.8	69.4	645 + j 97	1.19
200	5.00	5.99	165.0	79.8	1325 - j327	2.37

The sample performance values clearly show the general trend toward higher gain and a lower front-to-back ratio as we increase the ψ-angle. The table does not include ψ-angles below 10° because the forward gain is too small to be useful. As the table shows, if we widen the ψ-angle, the gain performance at the lower end of the passband decreases, although it gradually improves at the higher end of the operating range. The chief limiting factor at the widest ψ-angle sampled is the rapid decline in the front-to-back ratio.

Selecting a representative version of the boomless trapezoidal LPA is difficult in the absence of external specifications dictated by an intended application. For this collection, I used an arbitrary but not irrelevant criterion: minimum variation of certain key values across the passband. Two of the obvious performance categories are variations in forward gain and variations in the E-plane beamwidth. We may gather the required information by performing frequency sweeps from 50 to 200 MHz in 5-MHz increments. **Table 4** provides a summary of the sweep data used in making the selection.

Table 4. Sweep data summary, 50-200 MHz in 5-MHz increments: trapezoidal array: 20 elements/bay, α = 17°, τ = 0.9

1. Ψ = 10°

Category	Minimum	Maximum	Δ	Average
Gain dBi	3.05	7.64	4.59	5.97
Front-Back dB	7.27	17.85	10.58	14.26
E Beamwidth °	76.8	182.0	105.2	108.1

2. Ψ = 15°

Category	Minimum	Maximum	Δ	Average
Gain dBi	3.62	7.93	4.31	6.31
Front-Back dB	5.95	17.75	11.80	14.14
E Beamwidth °	76.6	179.4	102.8	108.6

3. Ψ = 20°

Category	Minimum	Maximum	Δ	Average
Gain dBi	4.48	8.20	3.72*	6.57
Front-Back dB	4.46	13.60	9.14	9.94
E Beamwidth °	73.6	170.0	96.4*	109.7

*Least variation across the passband of the trapezoidal group

4. ψ = 25°

Category	Minimum	Maximum	Δ	Average
Gain dBi	4.84	8.89	4.05	6.79
Front-Back dB	3.97	8.68	4.71	6.52
E Beamwidth °	65.4	173.4	108.0	111.6

One reason for not including variations in the front-to-back ratio among the criteria for the selection of an optimal ψ-angle is a function of using the 180° front-to-back value. This value changes more radically from one frequency to the next, even though the quartering rear sidelobes may show a relatively constant worst-case front-to-back ratio. In addition, the front-to-back ratio shows the smallest range of change when its values are also the lowest and the least desirable generally.

One general feature of trapezoidal zig-zag arrays is a very wide average E-plane beamwidth at every value of ψ. The E-plane beamwidth of a 3-element Yagi, for example, is about 60°, while the lowest average E-plane beamwidth for the set of trapezoidal LPAs is 50° wider. In addition, all versions of the trapezoidal LPA show considerable beamwidth variation across the operating passband.

Based on the fact that the LPA with a 20° value for ψ shows the least variation in both gain and beamwidth, I have selected it as the optimal version for this exercise. Nonetheless, the average front-to-back ratio is under 10 dB, and the upper passband end design remains suspect. I did not try to correct the design, since the values for α and τ will also be used with the boomless X-version of the LPA. The 20° value for ψ also shows a weakness in the correlation between the E-plane and the H-plane beamwidths. Since the array consists of 2 bays having a constant distance (relative to element length) between elements in the H-plane, there is a ψ-angle at which the bays show nearly equal beamwidth values in both planes. For the trapezoidal LPA, that angle is about 10°. **Fig. 9** provides a gallery of overlaid E-plane and H-plane free-space patterns at ψ=20° to demonstrate by how much the selected value for ψ

departs from equality. The data appendix will more clearly illustrate the rate of departure from equality of beamwidth as the value of ψ increases from 10° upward.

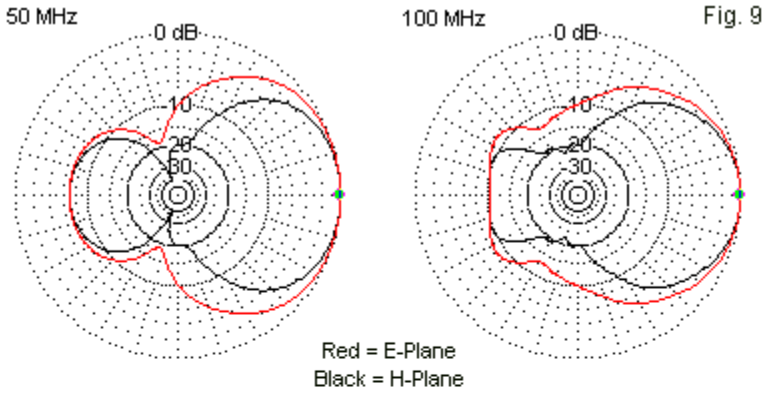

Fig. 9

20 Elements/Bay, Alpha = 17°, Tau = 0.9, Psi = 20°
Sample Free-Space E-Plane and H-plane Patterns

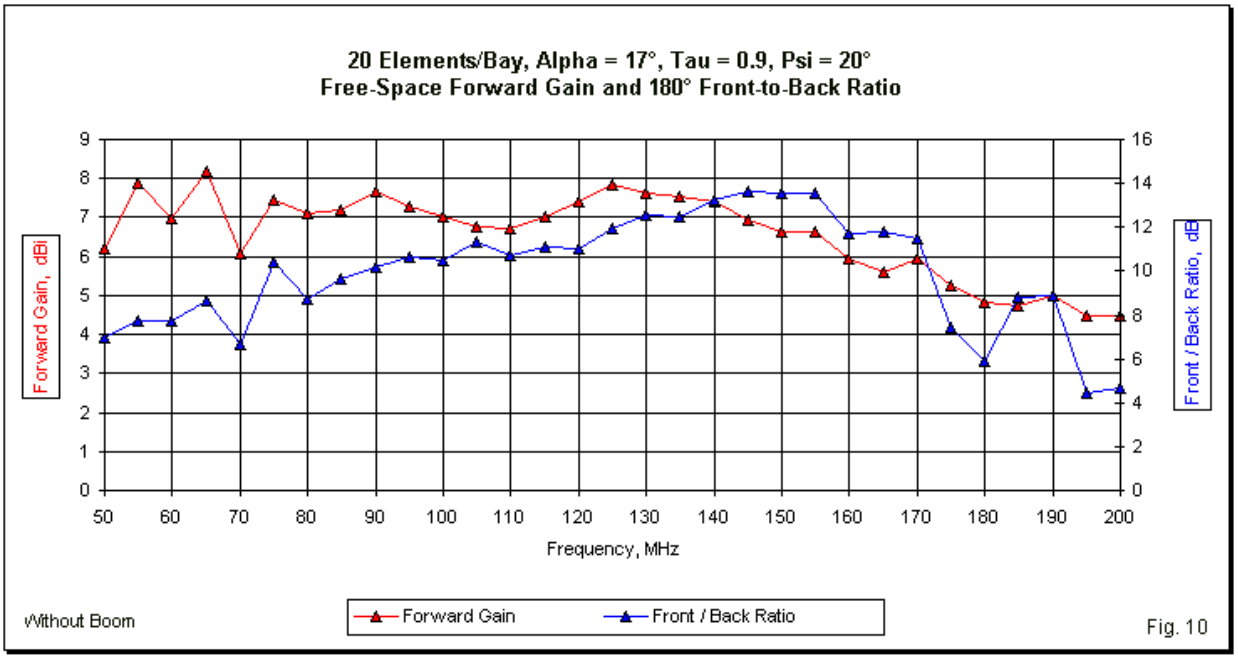

Fig. 10

Fig. 10 graphs the forward gain and the 180° front-to-back ratio across the passband. It shows a quite usable and relatively smooth set of values until the operating frequency exceeds about 175 MHz. The upper-end weakness and the need for redesign become apparent, especially from the front-to-back values. **Fig. 11** reinforces the design limitations by showing the rise in the feedpoint resistance and the 600-Ω SWR above the same break-point frequency. Since the degradation of performance affects virtually all categories of data in the upper 25 MHz of the design range, merely fussing with the feedpoint leads to improve the SWR value will not affect the basic capabilities of the trapezoidal LPA. Nothing short of adding elements toward the array vertex will do the job. We shall be interested in whether the X-version of the zig-zag LPA also requires such treatment.

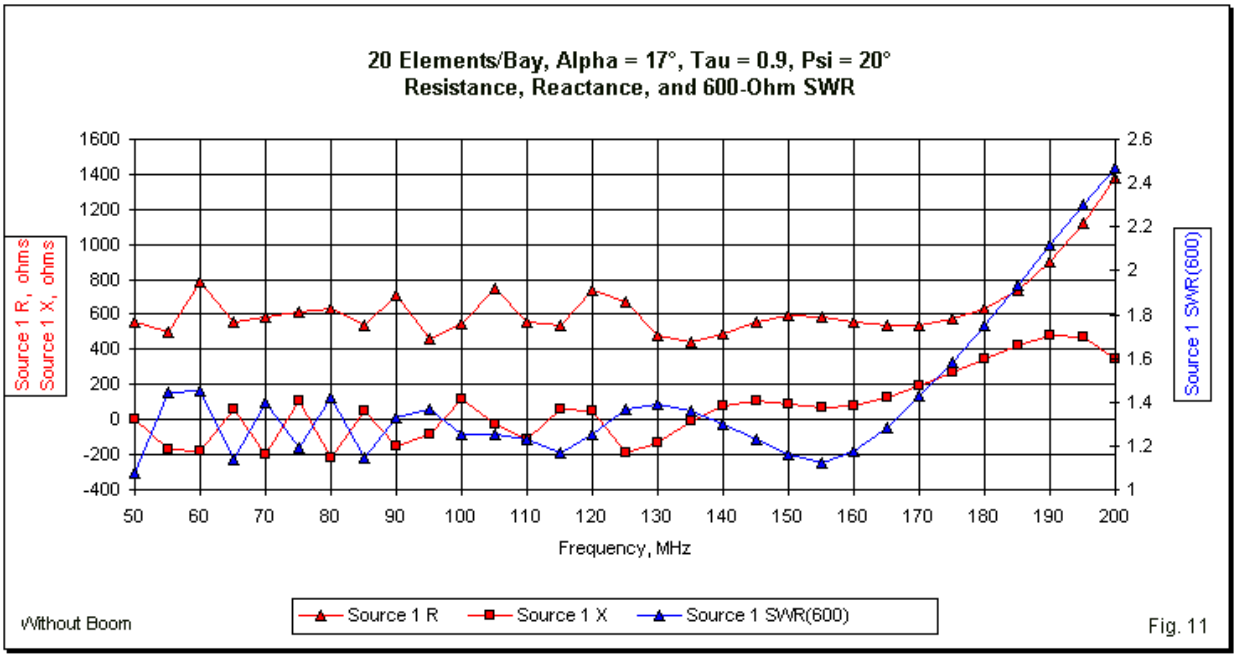

The absence of a boom in this set of trapezoidal arrays results in inferior performance in several ways relative to corresponding versions equipped with booms. For ψ-angles between 10° and 20°, the boomless gain deficit is just about 3-dB on average. Moreover, the sweep graphs for the entire collection of boom-equipped arrays are considerably smoother than those for corresponding boomless arrays. Finally, the pattern smoothness of the boom-equipped trapezoidal LPA show better control than do the patterns for any of the boomless versions. The boomless trapezoidal zig-zag LPA seems hardly worth the effort of building, especially in a wire version in which one may easily add a boom wire.

A Trapezoidal LPA with Boom from Amateur Archives

Early designs of trapezoidal arrays attempted to cover the television frequencies from 48 to 230 MHz and to include coverage of the amateur bands within that range. (For U.S. television viewers, the range began at about 54 MHz because this country did not use channel 1. Until the perfection of cable systems, channel-2 TVI from 6-meter transmitting equipment remained a perennial problem.) The quest also included mechanical constraints in terms of boom length. Therefore, both amateur and commercial designs resorted to fairly low values of τ and correspondingly wide values of α'. Most of the designs from the 1960s have disappeared from available literature. However, we may find samples of zig-zag LPA designs in Chapter 26 of the

1995 edition of *Rothammels Antennebuch*, edited by Alois Krischke, DJ0TR. See section 26.6, "Logarithmisch periodische Antennen für VHF und UHF," pp. 539-545. (Similar information appears beginning on p. 479 in the original edition of Karl Rothammel, Y21BK, *Antennenbuch* of 1984.) In this part of our work, we shall be most interested in the boom-equipped version that appears on pages 542-543 and is outlined in **Fig. 12**.

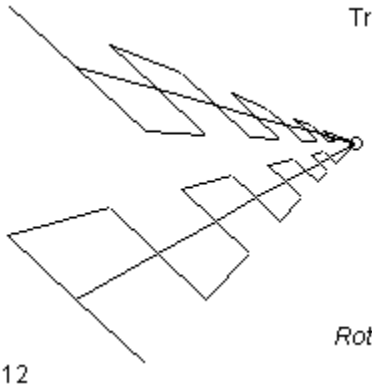

Trapezoidal LPA with Boom
Alpha = 60 Degrees
Psi = 45 Degrees
Tau = 0.707
8 Elements/Bay
48-230 MHz

Rothammels Antennembuch
pp. 542-543

Fig. 12

Zig-Zag Log-Periodic Antenna Elements											Fig. 13
DARC Trapezoidal Design		p.542									
Work Sheet		**Bold = User Entry**									
Tau		**0.707**								Sigma	0.127
Alpha	degrees	**60.00**	degrees	1.047	radians	1/2Alpha	0.524	tanAlpha	0.5774		0.127
F-low		**50.00**	MHz								
F-high		**200.00**	MHz								
L-long		3.00	meters	9.84	feet	118.11	inches				
Lhigh		0.75	meters	2.46	feet	29.53	inches				
L*1.6		0.47	meters	1.54	feet	18.45	inches				
Rv	Vertex R	2.60	meters	8.52	feet	102.29	inches				
Element	Ln	Ln/2	Rn	Element	Lfeet	Lft/2	Rfeet	Element	Linch	Lin/2	Rinch
1	3.000	1.500	2.598	*1*	9.84	4.92	8.52	*1*	118.11	59.06	102.29
2	2.121	1.061	1.837	*2*	6.96	3.48	6.03	*2*	83.50	41.75	72.32
3	1.500	0.750	1.299	*3*	4.92	2.46	4.26	*3*	59.04	29.52	51.13
4	1.060	0.530	0.918	*4*	3.48	1.74	3.01	*4*	41.74	20.87	36.15
5	0.750	0.375	0.649	*5*	2.46	1.23	2.13	*5*	29.51	14.75	25.56
6	0.530	0.265	0.459	*6*	1.74	0.87	1.51	*6*	20.86	10.43	18.07
7	0.375	0.187	0.324	*7*	1.23	0.61	1.06	*7*	14.75	7.38	12.77
8	0.265	0.132	0.229	*8*	0.87	0.43	0.75	*8*	10.43	5.21	9.03

Fig. 13 provides the basic dimensions of the array. The calculated value of σ is very close to optimal for the selected value of τ. The shortest element is self-resonant at a frequency well above the "1.6F" specified in the basic calculations, suggesting but not guaranteeing good performance at the high end of the operating range. The short forward element has a second potential advantage: as shown in the outline, the element is close enough to the vertex of the array to permit the use of short boom and final wire sections that join there. The only modification of the original design that occurs in the model is the use of 0.1" (2.54-mm) lossless wire as the conductor.

The array—using the relatively thin wire—shows a natural feedpoint impedance close to 300 Ω. **Table 5** provides sample performance data for the free-space model at 50, 100, 150, and 200 MHz.

Table. 5. Sample performance values: 8 elements/bay, α = 60°, τ = 0.707, ψ = 45°

Frequency MHz	Max. Gain dBi	Front-Back Ratio dB	E BW degrees	H BW degrees	Impedance R +/- jX Ω	300-Ω SWR
50	6.65	9.11	75.2	99.0	322 – j182	1.79
100	6.11	9.38	75.2	111.8	302 - j 18	1.06
150	6.07	8.94	75.6	101.8	297 - j 14	1.05
200	7.02	9.01	63.0	79.6	286 + j 5	1.05

As expected, the array performance shows a bias toward the high end of the band. The low end of the operating range shows a perfectly usable but nevertheless high 300-Ω SWR value relative to the other frequencies. The gain and front-to-back values are roughly comparable to those we might obtain from a 2-element driver-reflector Yagi at each sampled frequency.

The relatively low forward gain and modest front-to-back ratios suggest that the patterns at the sampled frequencies might show considerably more variation from one frequency to the next when compared to the patterns in **Fig. 4** for the main model with a τ of 0.9. The samples of free-space E-plane and H-plane in **Fig. 14** confirm the suspicion, especially with respect to the H-plane patterns.

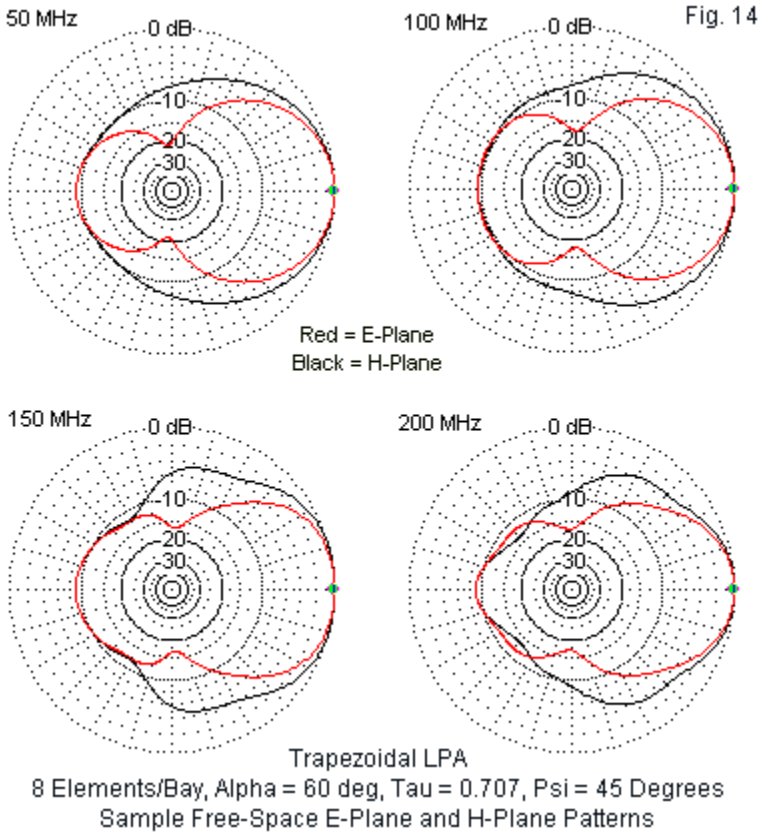

Fig. 14

Table 6 summaries a few of the key performance categories across the operating range. Perhaps the only worrisome value in the table is the wide range of E-plane beamwidth values across the passband exhibited by the array. Despite the use of a low value of τ (0.707) and a wide value of α' (60°), the array show no anomalous frequencies at the 5-MHz increment for the sweep scans shown in **Fig. 15** and **Fig. 16**.

Table 6. Frequency sweep summary: 50-200 MHz: 8 elements/bay, α = 60°, τ = 0.707, ψ = 45°

Category	Minimum	Maximum	Δ	Average
Gain dBi	5.10	7.02	1.92	6.34
Front-Back dB	6.90	11.75	4.85	9.67
E Beamwidth °	54.6	96.0	41.4	74.1

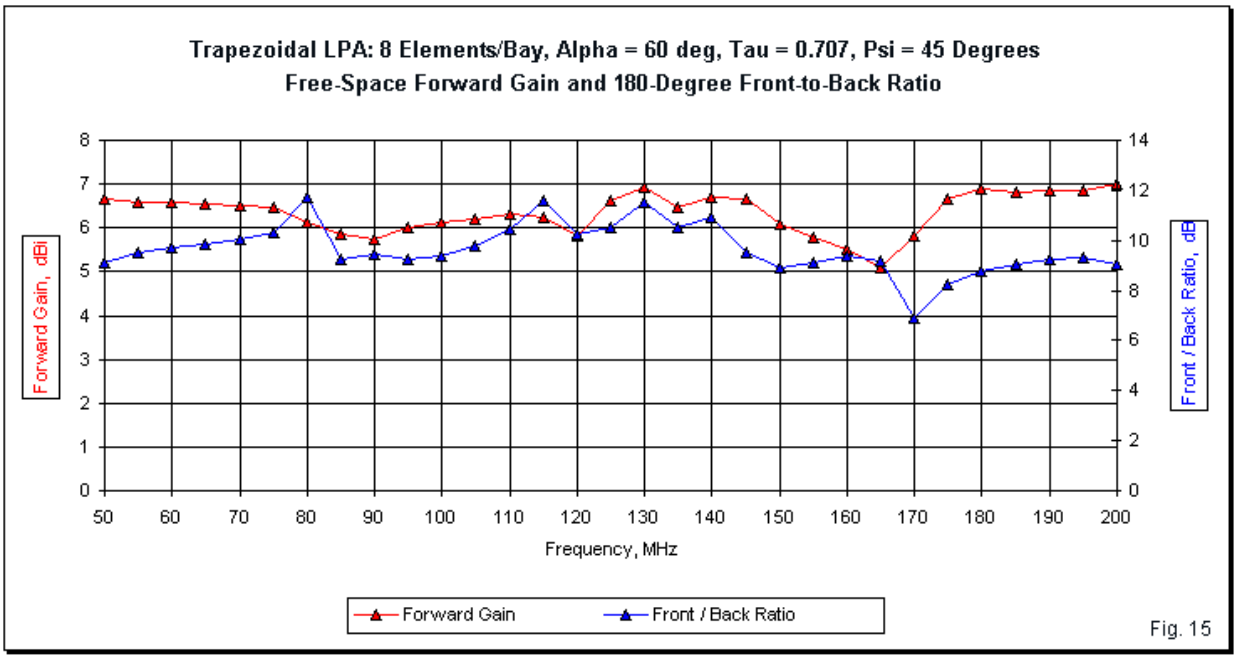

Fig. 15

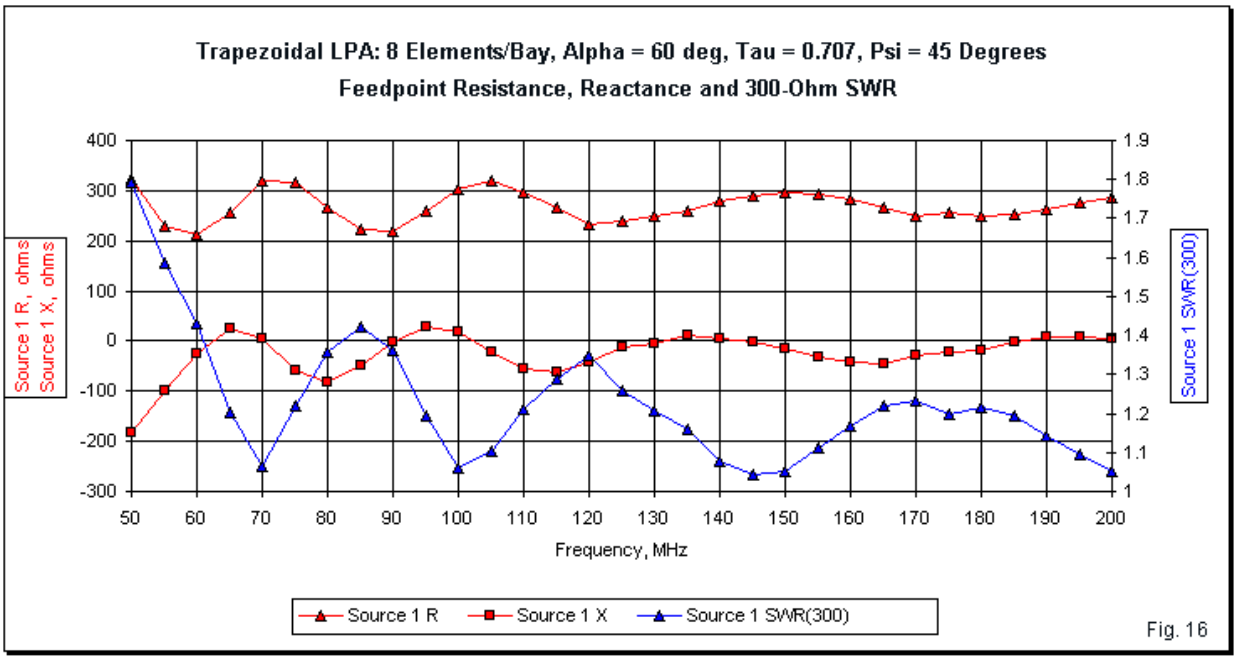

Fig. 16

One of the factors limiting array performance is the use of a very high value for ψ (45°). Early trapezoidal LPAs tended to use ψ-angles between 35° and 45° in order to assure the highest gain from the fewest elements. The present example is no exception. Without further

study, one cannot say if the design has used too high a value for ψ and hence reached a point where the gain begins to drop. Apart from this open question, using a large ψ-angle to obtain maximum gain results in mediocre front-to-back performance and equally mediocre pattern control, as indicated by the range of E-plane beamwidth variation. Since the model uses relatively thin elements to avoid modeling pitfalls, these questions will remain open to further study.

I did experiment with incremental increases in the wire diameter. At a fairly low diameter (4-mm), the gain suddenly jumped by about 5 dB with an accompanying drop in the feedpoint impedance to values in the 50-75-Ω range. Checking the average gain test (AGT) values showed that the source of the jumps was elevated wire interpenetration at angular junctions. Corrected for the AGT value in each case, the array show an average gain rise of less than 0.1-dB per millimeter increase in wire diameter. Corrected feedpoint impedance reports showed a gradual decline from 300 Ω toward 200 Ω.

The end result is that the classic zig-zag trapezoidal LPA design that we have reviewed yields fairly mediocre performance, although the performance does cover the entire passband and may be acceptable for some applications. One may design the zig-zag array using wide values of α' and low values of τ without encountering the anomalous frequencies of reversed patterns that are common to single-bay LPDAs trying to use the same values.

Conclusion to Part 2

Our brief journey through trapezoidal zig-zag LPAs has produced some interesting results. Using the relatively high τ of 0.9 and the relatively narrow α' of 17°--with accompanying low values for ψ—the trapezoidal array equipped with a boom replicates many of the performance characteristics of it solid-surface counterpart. It is capable of exceeding the gain of a single-bay LPDA using the same design parameters, but falls short of a 2-bay LPDA. The front-to-back ratio is good, if we compare it to typical Yagi performance, but falls short of what we may obtain from an LPDA. The performance and impedance curves are generally quite smooth across the operating passband. In short, the boom-equipped trapezoidal LPA is a very serviceable array where the builder prefers not to wrestle with a phase line. In contrast, the theoretically possible boomless version of the trapezoidal array has significantly lesser performance that hardly merits construction.

Classic early trapezoidal zig-zag designs—with lower values of τ and much wider values of α'—lack a convenient summery evaluation. Although relatively modest in general performance, they can provide that performance over a wide frequency span and may prove to be adequate for some applications. Optimizing such designs within their avowed limitations in boom length is a task outside the scope of this study.

Theoretically, the X or saw tooth zig-zag LPA is the equivalent of the trapezoidal array. To what degree theory holds up in practice—using our standard design parameters—will be the subject of the final part in this series.

A Tale of Three LPAs: Some Notes on Zig-Zag Log-Periodic Arrays
3. The X or Saw Tooth Zig-Zag LPA

L. B. Cebik, W4RNL

The trapezoid was not the only solid-surface element shape to have a wire-outline analog in the development of LPAs. Performing similarly to the trapezoid was the saw tooth shape, shown in wire-outline single-bay form in **Fig. 1**. Like the trapezoid, solid-surface forms used a central boom composed of a line that grew wider as the distance from the vertex increased. The wire-outline version reduced the central line to the diameter of the wire itself. Folding two bays together produced a directional beam. From above, the pattern of elements formed the series of Xs that yields the casual array name.

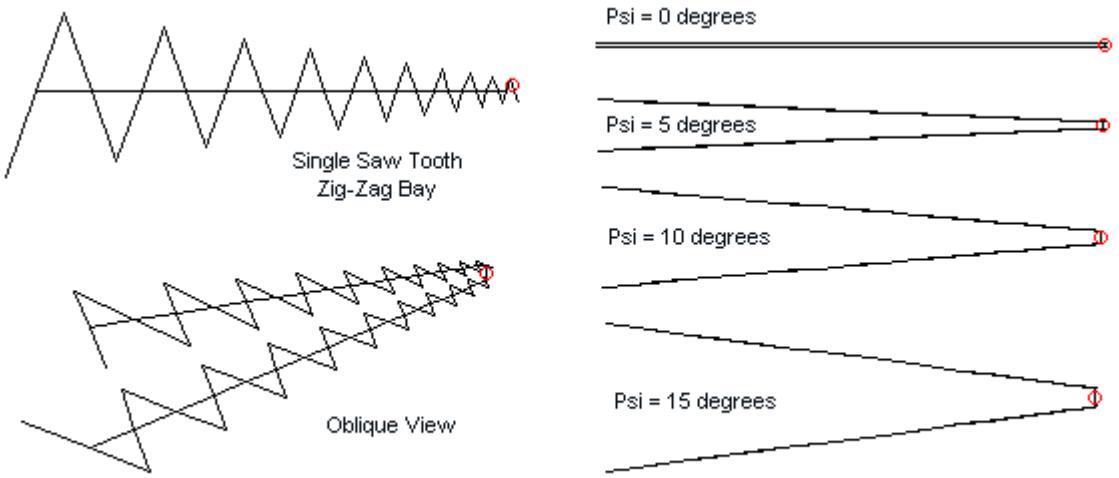

General Outlines of X (Saw Tooth) Zig-Zag LPAs with Booms

Fig. 1

In the early 1960s, J. W. Carr discovered that he could remove the central boom and still have a useful beam. Therefore, we shall have to see whether boomless X LPAs are more or less successful than boomless trapezoidal arrays. Finally, we shall look at two amateur examples of X LPAs using far less stringent design criteria than the ones we shall employ in our main comparative study.

As we did for the LPDA and the trapezoidal zig-zag array, we shall impose design parameters that best assure us of reasonable performance. Even though the arrays are too long to be practical for most cases, they serve modeling needs well. When $\tau = 0.9$, $\sigma = o.167$, and $\alpha' = 17°$, we obtain worthwhile performance over all or most of the 50-200 MHz operating passband. The ψ-angle will be subject to variation to explore any differences that it makes to performance. The limits of NEC modeling dictate that we use rather thin wire, in this case, 0.1" (2.54-mm) lossless wire for all elements. Each bay will use 20 elements, resulting in fairly sizable models. As a review, **Fig. 2** provides the spreadsheet page that indicates the dimensions used in the models.

The zig-zag X LPA handles the dimensions in a slightly different manner than did the LPDA and the trapezoidal arrays. If we think of a Cartesian axis as the centerline of the model, the earlier LPAs defined each element as extending for Ln/2 on both sides of the centerline. The saw tooth zig-zag alters the arrangement such that the first element extends from –L1/2 to

+L2/2. In the process, it also moves forward toward the vertex from R1 to R2. The next element reverses and increments the process.

Zig-Zag Log-Periodic Antenna Elements											Fig. 2
Work Sheet		**Bold = User Entry**									
Tau		**0.90**								Sigma	0.167
Alpha'	degrees	**17.00**	degrees	0.297	radians	1/2Alpha'	0.148	tanAlpha	0.1495		0.167
F-low		**50.00**	MHz								
F-high		**200.00**	MHz								
L-long		3.00	meters	9.84	feet	118.11	inches				
Lhigh		0.75	meters	2.46	feet	29.53	inches				
L*1.6		0.47	meters	1.54	feet	18.45	inches				
Rv	Vertex R	10.04	meters	32.93	feet	395.15	inches				
Element	Ln	Ln/2	Rn	Element	Lfeet	Lft/2	Rfeet	Element	Linch	Lin/2	Rinch
1	3.00	1.50	10.04	*1*	9.84	4.92	32.93	*1*	118.11	59.06	395.15
2	2.70	1.35	9.03	*2*	8.86	4.43	29.64	*2*	106.30	53.15	355.63
3	2.43	1.22	8.13	*3*	7.97	3.99	26.67	*3*	95.67	47.83	320.07
4	2.19	1.09	7.32	*4*	7.18	3.59	24.01	*4*	86.10	43.05	288.06
5	1.97	0.98	6.59	*5*	6.46	3.23	21.60	*5*	77.49	38.75	259.26
6	1.77	0.89	5.93	*6*	5.81	2.91	19.44	*6*	69.74	34.87	233.33
7	1.59	0.80	5.33	*7*	5.23	2.62	17.50	*7*	62.77	31.38	210.00
8	1.43	0.72	4.80	*8*	4.71	2.35	15.75	*8*	56.49	28.25	189.00
9	1.29	0.65	4.32	*9*	4.24	2.12	14.17	*9*	50.84	25.42	170.10
10	1.16	0.58	3.89	*10*	3.81	1.91	12.76	*10*	45.76	22.88	153.09
11	1.05	0.52	3.50	*11*	3.43	1.72	11.48	*11*	41.18	20.59	137.78
12	0.94	0.47	3.15	*12*	3.09	1.54	10.33	*12*	37.06	18.53	124.00
13	0.85	0.42	2.83	*13*	2.78	1.39	9.30	*13*	33.36	16.68	111.60
14	0.76	0.38	2.55	*14*	2.50	1.25	8.37	*14*	30.02	15.01	100.44
15	0.69	0.34	2.30	*15*	2.25	1.13	7.53	*15*	27.02	13.51	90.40
16	0.62	0.31	2.07	*16*	2.03	1.01	6.78	*16*	24.32	12.16	81.36
17	0.56	0.28	1.86	*17*	1.82	0.91	6.10	*17*	21.89	10.94	73.22
18	0.50	0.25	1.67	*18*	1.64	0.82	5.49	*18*	19.70	9.85	65.90
19	0.45	0.23	1.51	*19*	1.48	0.74	4.94	*19*	17.73	8.86	59.31
20	0.41	0.20	1.36	*20*	1.33	0.66	4.45	*20*	15.95	7.98	53.38

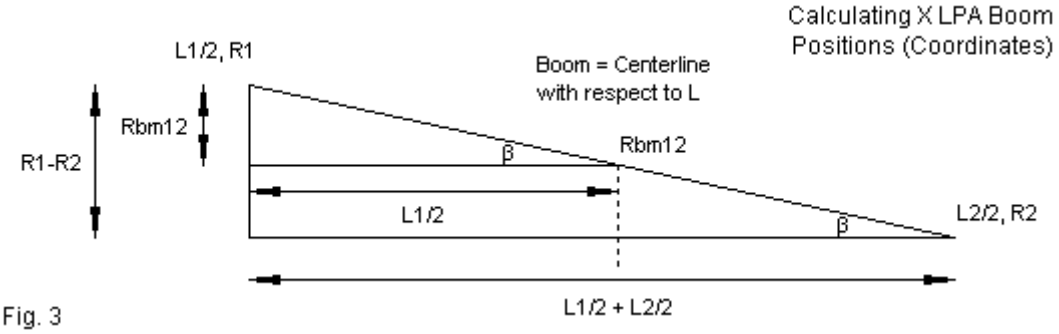

Fig. 3

Fig. 3 shows the first element along with a simple solution to the question of where to position the junction of the element with the boom at the array centerline. The position of Rbm12, the boom section that extended from element 1 to element 2, relative to the array vertex is proportional to the ratio of L1/2 to L1/2+L2/2. We may calculate the position of Rbm12 either from the proportionality of congruent triangles or by obtaining the tangent of the angle shown as β in the diagram. Once we have the position of the first boom junction, we may find all other junctions by multiply successively by the value of τ. **Fig. 4** provides the calculated values of Rbm for the X LPAs equipped with booms. The single-bay and the oblique double-bay diagrams in **Fig. 1** should suffice to confirm the accuracy of the method.

X-LPA Boom Calculations			Fig. 4
Adjacent	2.85		
Opposite	1.003673		
tanBeta	0.352166		
Rbm-n	9.508485		
Boom	Rbm-m	Rbm-ft	Rbm-in
1-2	9.508	31.20	374.35
2-3	8.558	28.08	336.91
3-4	7.702	25.27	303.22
4-5	6.932	22.74	272.90
5-6	6.239	20.47	245.61
6-7	5.615	18.42	221.05
7-8	5.053	16.58	198.94
8-9	4.548	14.92	179.05
9-10	4.093	13.43	161.15
10-11	3.684	12.09	145.03
11-12	3.315	10.88	130.53
12-13	2.984	9.79	117.47
13-14	2.685	8.81	105.73
14-15	2.417	7.93	95.15
15-16	2.175	7.14	85.64
16-17	1.958	6.42	77.08
17-18	1.762	5.78	69.37
18-19	1.586	5.20	62.43
19-20	1.427	4.68	56.19
20-21	1.284	4.21	50.57

As with earlier double-bay models, we shall not try to extend forward leads all the way to the vertex. As **Fig. 4** indicates, the distance from the forward-most element to the vertex is several times longer than the distance between elements. Directly connecting the booms with a single direct lead provides the most economical model with no harmful effects on the reported data.

X LPAs with Booms.

X or saw tooth LPAs equipped with central booms have current magnitude distribution curves that are as difficult to decipher as their trapezoidal counterparts. **Fig. 5** shows the distribution curve set for one of the LPAs at 50 MHz. In the side view of the array, the nearly level lines represent currents on the boom, while the more curved lines represent currents on the angular elements. The face view of the array's upper bay shows only the element currents.

Although more difficult to see due to the angularity of the elements, the boom-equipped X LPA preserves some, if not most, of the properties associated with the solid-surface bay that the wire-outline version approximates. Current magnitude may abruptly change as an element intersects the boom, since the currents on each side are associated with a different saw-tooth shape. In the side view, the most active region in terms of peak current magnitude for the X LPA extends for a considerable distance toward the vertex. However, the element angles and the disparate collection of wire sections involved do not allow us to see fine detail.

Fig. 1 shows the range of ψ-angles that we shall examine for X LPAs with booms. The data will clarify why I limited the range to 0° to 20° in 5° increments. We may sample the performance at each ψ-angle using the data in **Table 1**, which provides values for 50, 100, 150, and 200 MHz.

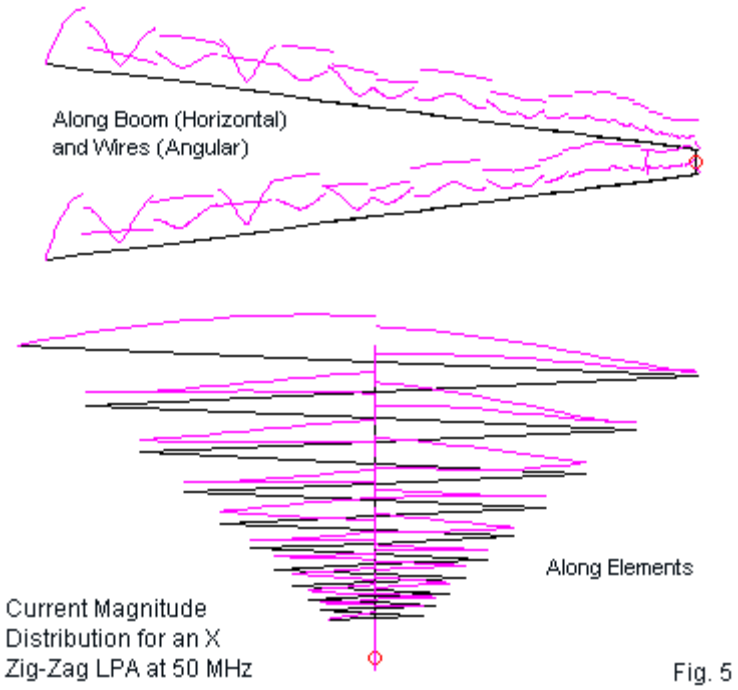

Fig. 5

Table 1. Sample performance values of X zig-zag LPAs using various ψ-angles

1. 20 elements/bay, α = 17°, τ = 0.9, ψ = 0° (flat array, 4" separation between bays)

Frequency MHz	Max. Gain dBi	Front-Back Ratio dB	E BW degrees	H BW degrees	Impedance R +/- jX Ω	250-Ω SWR
50	7.28	15.70	64.2	99.2	276 - j 26	1.15
100	8.13	30.62	64.6	95.6	270 - j 33	1.16
150	8.29	27.14	64.2	94.6	246 - j 23	1.10
200	8.43	22.34	63.0	91.8	178 - j 12	1.41

2. 20 elements/bay, α = 17°, τ = 0.9, ψ = 5°

Frequency MHz	Max. Gain dBi	Front-Back Ratio dB	E BW degrees	H BW degrees	Impedance R +/- jX Ω	250-Ω SWR
50	7.64	11.96	63.5	90.2	252 - j 78	1.36
100	8.64	29.77	63.8	88.0	267 - j 39	1.18
150	8.70	26.57	64.0	88.8	241 - j 20	1.09
200	8.79	22.60	62.4	86.8	175 - j 7	1.44

3. 20 elements/bay, α = 17°, τ = 0.9, ψ = 10°

Frequency MHz	Max. Gain dBi	Front-Back Ratio dB	E BW degrees	H BW degrees	Impedance R +/- jX Ω	300-Ω SWR
50	8.25	9.06	62.8	77.0	324 – j138	1.56
100	9.38	23.42	64.0	76.3	307 - j 1	1.02
150	9.44	22.14	63.4	75.6	268 +j 44	1.21
200	9.27	18.23	63.0	75.8	197 + j 93	1.75

4. 20 elements/bay, α = 17°, τ = 0.9, ψ = 15°

Frequency MHz	Max. Gain dBi	Front-Back Ratio dB	E BW degrees	H BW degrees	Impedance R +/- jX Ω	300-Ω SWR
50	8.72	6.87	63.0	63.1	368 – j185	1.79
100	9.52	18.88	68.0	64.6	381 + j 38	1.30
150	9.65	18.81	65.8	63.2	303 + j 94	1.36
200	9.48	15.81	62.4	62.0	230 + j202	2.21

As we increase the value of ψ, the reference impedance for general SWR values increases from 250 Ω to 300 Ω. One of the two major limiting factors in X LPA performance is the rising reactance value as the ψ-angle increases, resulting in SWR values that exceed the normal 2:1 limit that we often employ as a standard. The other limitation is the gain and front-to-back performance at the low end of the passband. The rising gain value at 50 MHz does not keep pace with the rapidly declining front-to-back value at that frequency. We may re-affirm these general impressions using summary frequency sweep data, shown in **Table 2**.

Table 2. Frequency sweep summery of X zig-zag LPAs using various ψ-angles from 50 to 200 MHz

1. ψ = 0°

Category	Minimum	Maximum	Δ	Average
Gain dBi	7.28	8.44	1.16	8.17
Front-Back dB	15.70	34.21	18.51	27.84
E Beamwidth °	63.0	65.5	2.5	64.3

2. ψ = 5°

Category	Minimum	Maximum	Δ	Average
Gain dBi	7.64	8.84	1.20	8.64
Front-Back dB	11.96	30.93	18.97	26.87
E Beamwidth °	62.4	64.6	2.2*	63.5

*Least variation across the passband of the group.

3. ψ = 10°

Category	Minimum	Maximum	Δ	Average
Gain dBi	8.25	9.52	1.27	9.31
Front-Back dB	9.06	25.85	17.69	21.75
E Beamwidth °	62.6	65.4	2.8	63.8

4. ψ = 15°

Category	Minimum	Maximum	Δ	Average
Gain dBi	8.72	9.87	1.15*	9.56
Front-Back dB	6.87	22.01	15.14	17.49
E Beamwidth °	62.1	69.8	7.7	65.5

*Least variation across the passband of the group.

Because the data with the smallest range of variation does not focus upon a single ψ-angle, my selection of a representative array for graphical presentation is somewhat arbitrary. I selected the version in which ψ = 5° for several reasons. The SWR remains below 2:1 across the operating range. The average front-to-back ratio has not begun its rapid decline. As well, the E-plane beamwidth shows the least variation across the operating range. Indeed, the patterns shown in **Fig. 6** display good control, allowing for the lesser performance of the X LPA

at the low end of the operating range. Any implementation of this array would naturally wish to begin with a longer rear element.

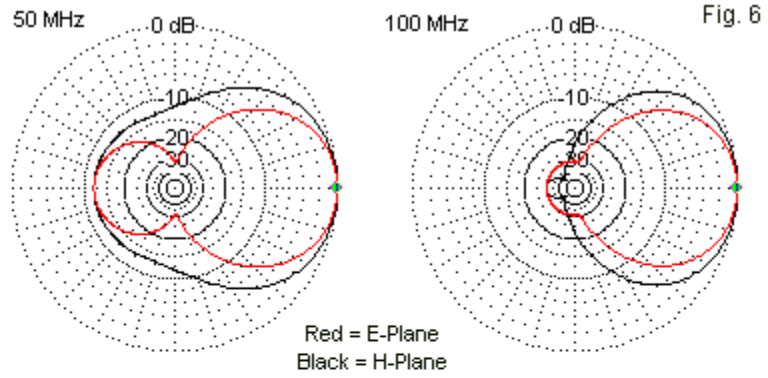

Fig. 6

20 Elements/Bay, Alpha = 17°, Tau = 0.9, Psi = 5°
Sample Free-Space E-Plane and H-plane Patterns

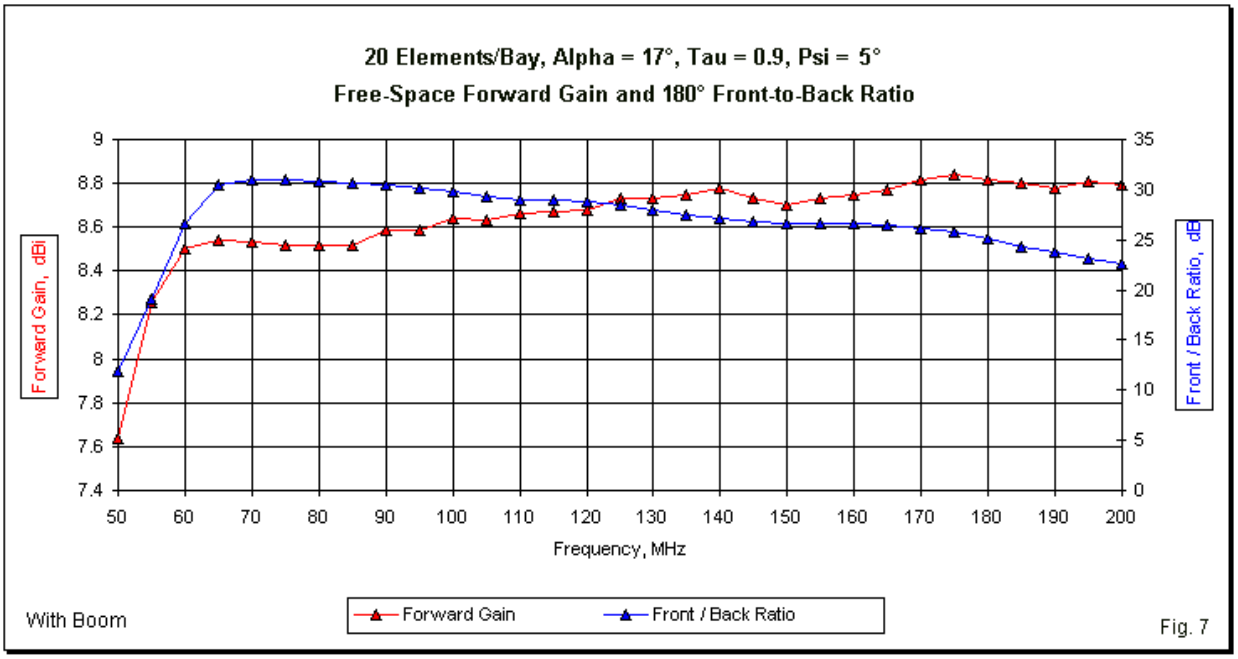

Fig. 7

The sweep graph of free-space forward gain and 180° front-to-back ratio confirms the general decline of performance below 60 MHz. Otherwise, the curves are exceptionally smooth. Equally smooth are the impedance curves (resistance, reactance, and 250-Ω SWR) shown in **Fig. 8**. Below 55 MHz, we can see a sudden turn in all of the values, although the sweep limits do not inform us of where the curves go below 50 MHz. Nevertheless, the combination of sweep performance graphs suggests that the span of good impedance performance is greater than the span of peak gain and front-to-back performance.

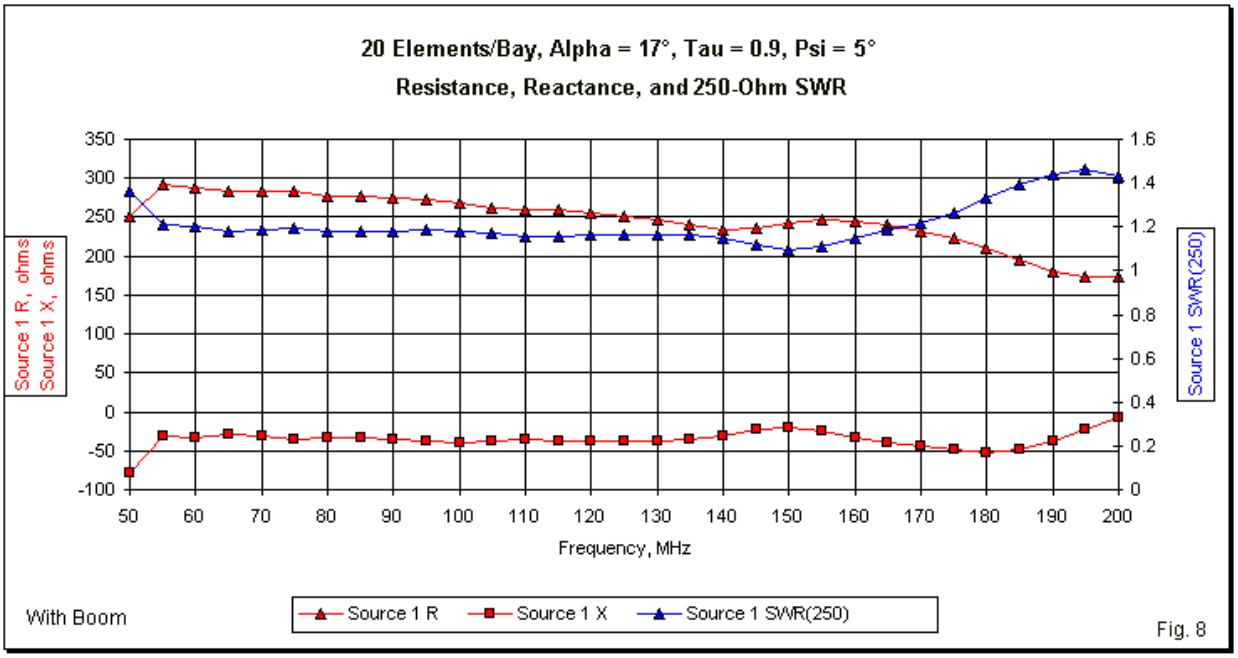

Fig. 8

Very little distinguishes the performance of boom-equipped trapezoidal LPAs and their X counterparts, once we compensate for any deficiencies at one or the other end of the operating passband. One might profitably study the corresponding data for all ψ-angles for both types of arrays in the data appendix.

X LPAs without Booms

Carr's innovation of removing the central boom from a zig-zag saw tooth bay resulted in a usable configuration. Unlike the boomless trapezoidal array, the boomless X array saw considerable use, especially in magazine plans for home-built television antennas. Therefore, we shall examine this type of array, using our standard design parameters, to see how it measures up against both the trapezoidal version and against the X LPA with a central boom.

The dimensions and design values are the same as used for the trapezoidal array and outlined in **Fig. 2**. $\tau = 0.9$ and $\alpha' = 17°$. The only difference is the omission of the side wires. Each element extends from a point defined by the limit of one element to the opposite limit determined by the value of τ applied to the initial limit. The result is two opposing bays of saw tooth elements that form a series of Xs when viewed directly from above or below. Like the trapezoidal array, the two bays have an angular separation determined by experimentally selected values of ψ. The models of the X LPAs created a wire connecting the free ends of the innermost elements on which to place the model source, since alternative lead arrangements created no significant changes in performance.

Because the X-version of the zig-zag LPA has no side wires, we may more easily see the current magnitude distribution along the wires. In **Fig. 9**, the blue dots represent wire ends and, therefore, changes in the wire direction. The green sections are the intervening wires as seen from the array side. The accompanying general outline of this model, which uses a ψ of 10°, provides an orientation to the wires from an oblique angle.

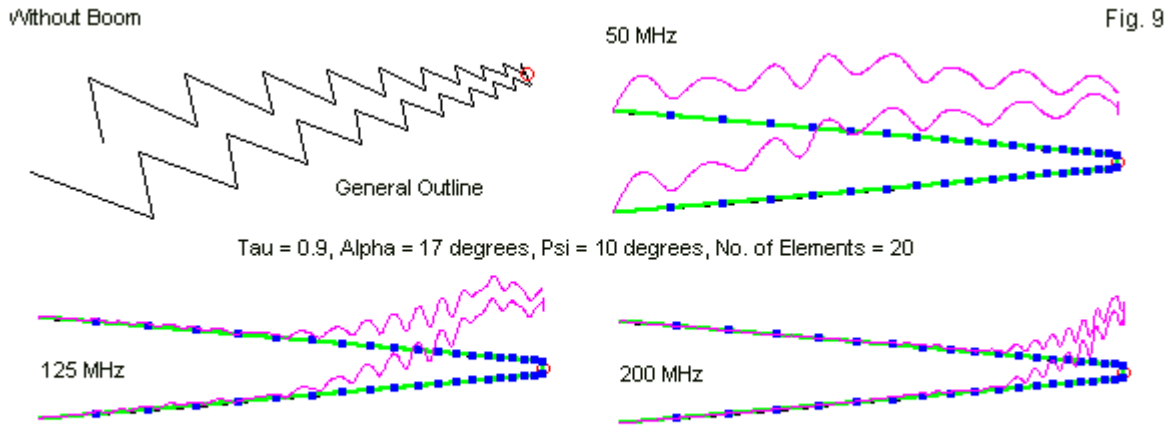

General Outline and Current Magnitude Distribution Along an X Zig-Zag Array at 3 Frequencies within the Operating Range

Like the trapezoidal zig-zag array, the X LPA shows the same tendency toward a maximum current peak along each bay that is far forward of the corresponding element on an LPDA. As well, the absence of wire free ends reveals that the current minimums do not necessarily occur at the points where the wire changes direction. See **Fig. 10**, which shows significant differences in the current curves relative to the version in **Fig. 5**. Note especially that some of the parallels to the current of solid-surface elements are missing.

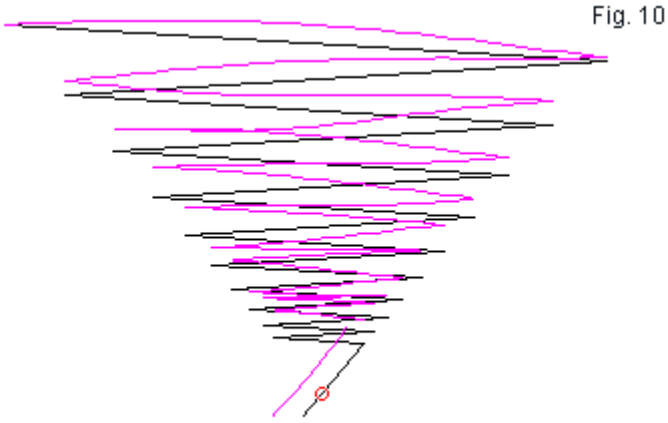

50-MHz Current Magnitude Distribution Along One Element Bay of an X Zig-Zag LPA

To allow more detailed comparisons between the trapezoidal and the X LPAs, we may look at sample data at 50, 100, 150, and 200 MHz for the range of ψ-angles covered by this initial exploration. The range of ψ-angles for the X LPA is not the same as for the trapezoidal counterpart. X arrays have been successfully used when ψ = 0°, with a small separation between the bays. In fact, we shall later discover that a ψ of 10° may be the most optimal angle

between bays when measured by the criteria used to select the optimal trapezoidal array. Therefore, the sample includes ψ-angles of 0°, 10°, 15°, and 20°. **Table 3** provides the results of the sampling.

Table 3. Sample performance values: X (saw tooth) array: 20 elements/bay, α = 17°, τ = 0.9

1. ψ = 0° (flat array, 4" separation between bays)

Frequency MHz	Max. Gain dBi	Front-Back Ratio dB	E BW degrees	H BW degrees	Impedance R +/- jX Ω	600-Ω SWR	500-Ω SWR
50	6.51	11.66	84.6	117.4	477 + j 61	1.29	1.14
100	6.34	12.15	87.4	115.2	446 + j 57	1.37	1.18
150	6.86	15.69	79.6	103.4	504 – j119	1.32	1.27
200	5.79	16.53	107.2	134.0	301 + j 18	2.00	1.67

2. ψ = 5°

Frequency MHz	Max. Gain dBi	Front-Back Ratio dB	E BW degrees	H BW degrees	Impedance R +/- jX Ω	600-Ω SWR
50	7.42	11.42	76.4	99.0	573 – j160	1.32
100	7.50	14.18	73.2	93.4	458 - j 98	1.39
150	6.95	16.78	77.2	98.8	577 - j 6	1.04
200	6.35	18.14	100.4	124.8	307 - j 15	1.96

3. ψ = 10°

Frequency MHz	Max. Gain dBi	Front-Back Ratio dB	E BW degrees	H BW degrees	Impedance R +/- jX Ω	600-Ω SWR
50	7.90	9.46	74.2	83.8	754 + j 78	1.29
100	7.32	18.82	82.4	91.4	619 - j 99	1.18
150	7.04	17.72	83.4	95.6	592 + j 82	1.15
200	7.21	16.69	90.2	96.6	332 - j 30	1.81

4. ψ = 15°

Frequency MHz	Max. Gain dBi	Front-Back Ratio dB	E BW degrees	H BW degrees	Impedance R +/- jX Ω	600-Ω SWR
50	8.34	7.53	73.4	69.0	726 + j 217	1.46
100	7.23	9.58	88.4	79.0	658 - j 87	1.18
150	7.27	13.34	89.6	79.6	672 + j 94	1.21
200	7.50	15.01	91.0	79.8	355 + j 20	1.69

5. ψ = 20°

Frequency MHz	Max. Gain dBi	Front-Back Ratio dB	E BW degrees	H BW degrees	Impedance R +/- jX Ω	600-Ω SWR
50	8.79	6.11	73.8	56.8	776 + j 302	1.66
100	6.48	4.12	106.8	71.2	629 - j 56	1.11
150	7.44	5.23	98.8	55.2	693 + j 33	1.16
200	7.71	7.60	92.0	68.0	440 + j 95	1.43

As was the case with the trapezoidal LPA, the X version of the array shows increasing gain and decreasing front-to-back performance as we increase the ψ-angle. Also in concert with the trapezoidal version, the X array shows an approximate feedpoint resistance of about 600 Ω. The one exception to this rule is the flat version; here the impedance is closer to 500 Ω. The

entry for that version alone provides SWR values relative to both 600 Ω and 500 Ω. Notably, none of the 200-MHz SWR values exceeds 2:1, and the performance does not radically diminish at 200 MHz, as it did in the case of the trapezoidal LPA. Only the flat version of the array shows a noticeable decrease in forward gain at the highest frequency within the operating range.

The alternative way in which we may compare data both within the group of X LPAs and between the trapezoidal and X types is to summarize the sweep data from 50 to 200 MHz. The X LPA information appears in **Table 4**. There are three striking features within the table. First, the optimal ψ-angle is about 10°, if we use the criteria of the smallest change in gain and the smallest change in the E-plane beamwidth across the operating passband. We might have as easily selected the version in which ψ = 5°, since the overall rate of performance change with changes in the value of ψ is quite small. The selected ψ-angle angle is about half the value required by the trapezoidal array.

Table 4. Sweep data summary, 50-200 MHz in 5-MHz increments: X (saw tooth) array: 20 elements/bay, α = 17°, τ = 0.9

1. Ψ = 0° (flat array, 4" separation between bays)

Category	Minimum	Maximum	Δ	Average
Gain dBi	4.67	7.32	2.65	6.23
Front-Back dB	8.04	17.18	9.14	12.70
E Beamwidth °	74.2	116.4	42.2	91.0

2. ψ = 5°

Category	Minimum	Maximum	Δ	Average
Gain dBi	6.19	7.53	1.34*	6.87
Front-Back dB	9.79	18.26	8.47	15.10
E Beamwidth °	87.2	124.8	37.6	107.9

*Least variation across the passband of the group.

3. Ψ = 10°

Category	Minimum	Maximum	Δ	Average
Gain dBi	6.00	7.90	1.90	7.30
Front-Back dB	9.44	19.78	10.34	16.31
E Beamwidth °	73.0	107.6	34.6*	84.0

*Least variation across the passband of the group.

4. Ψ = 15°

Category	Minimum	Maximum	Δ	Average
Gain dBi	5.27	8.62	3.35	7.49
Front-Back dB	7.51	18.06	10.55	12.26
E Beamwidth °	65.6	134.2	68.6	86.5

5. ψ = 20°

Category	Minimum	Maximum	Δ	Average
Gain dBi	5.38	9.21	3.83	7.61
Front-Back dB	2.85	10.04	7.19	6.10
E Beamwidth °	45.6	158.2	112.6	88.8

In addition, the 10° ψ-angle also yields a very close coincidence between the E-plane and the H-plane beamwidths, as shown in the gallery of patterns in **Fig. 11**. Indeed, when ψ = 10°, we find a near symmetry in the patterns for the two planes. In general, the X array yields narrower beamwidths than the trapezoid.

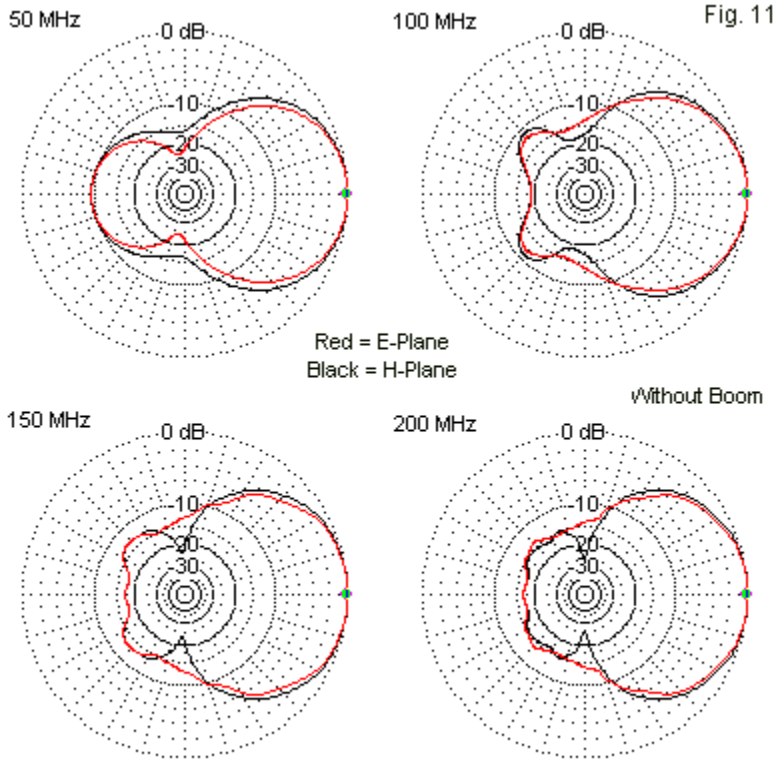

Fig. 11

Without Boom

20 Elements/Bay, Alpha = 17°, Tau = 0.9, Psi =10°
Sample Free-Space E-Plane and H-plane Patterns

Second, average gain across all versions of the boomless X array tends to be higher by an average of about 1 dB than the gain of the boomless trapezoidal LPA. Even with a ψ-angle of 0°, that is a flat array, the X LPA is capable of significant gain and a good front-to-back ratio, which goes some distance to explaining the popularity of the design in home-built TV antennas. The third notable factor is less debatable, since the range of change in both gain and the E-plane beamwidth is much smaller among the boomless X LPAs than among the trapezoidal counterparts. The general impression left by the X versions of the LPA is that they provide better pattern control across the operating bandwidth than do the trapezoidal arrays.

Fig. 13 and **Fig. 14** provide sweep graphs for the version of the array where ψ = 10°. Graphs for the other versions of the X LPA appear in the data appendix document. The sweep of forward gain and the 180° front-to-back ratio reveals that the design might benefit from a slightly longer rear element. We also saw this feature in the corresponding sweep for the trapezoidal array, but there, the effect was more pronounced at the low end of the operating range. At the upper end of the range, the gain and the front-to-back ratio show no significant decline, although the beamwidth tends to grow slowly with the operating frequency.

In common with the trapezoidal array, the X LPA SWR increases as the operating frequency exceeds about 185 MHz. However, the rate of increase is much smaller than we encountered with the trapezoidal array. Part of the reason for the slower rise in the 600-Ω SWR is the fact

that it is due to a declining feedpoint resistance, in contrast to the trapezoidal array that showed a rapid rise in the feedpoint resistance at the upper end of the passband.

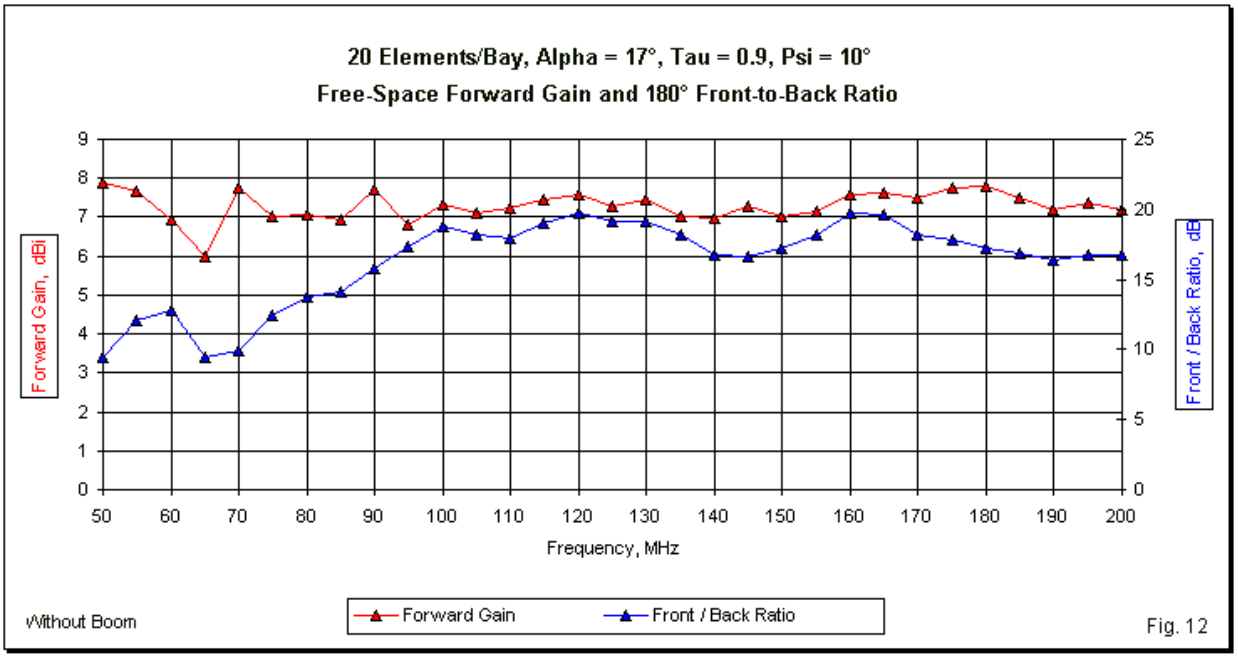

Fig. 12

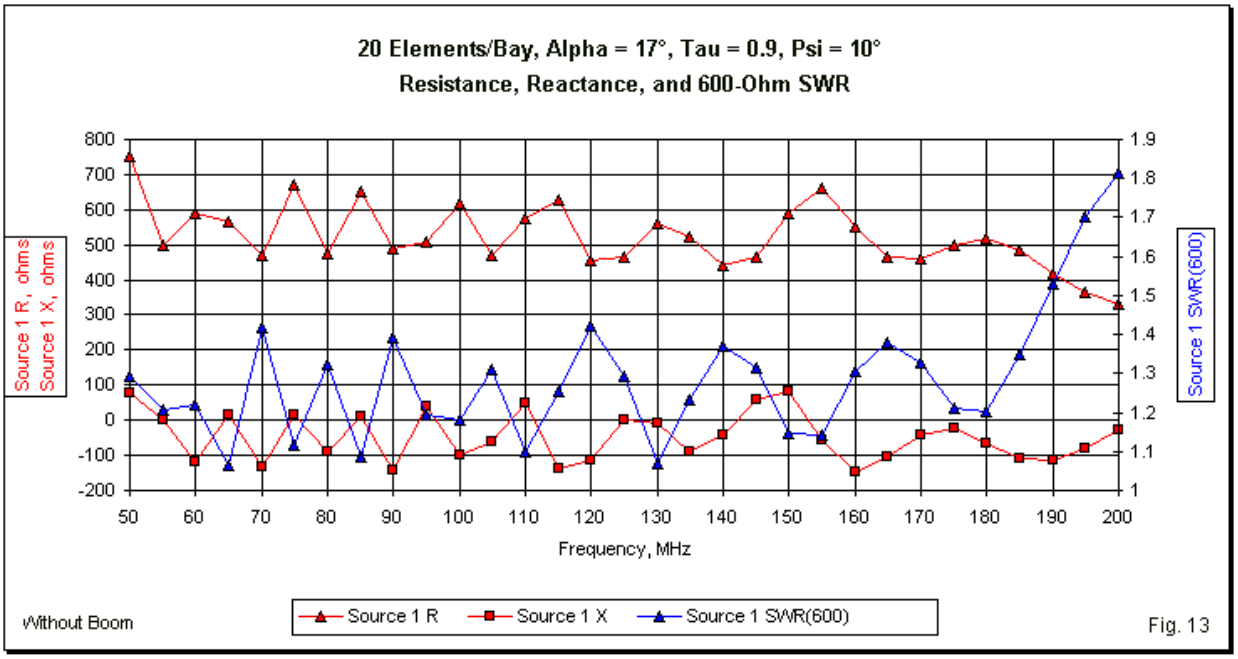

Fig. 13

The boomless X or saw tooth LPA leaves the impression that it is generally superior to the trapezoidal configuration in terms of performance at both ends of the operating passband and in terms of pattern control. The optimal configuration requires a smaller ψ-angle, and even a flat version is capable of reasonably good performance. The boomless X LPA still averages about a 2-dB gain deficit relative to either type of array when equipped with a boom and a 1-dB deficit relative to a single-bay LPDA. The boomless X LPA also has a somewhat lower front-to-back

average value than its boom-equipped counterpart. Still, if we measure simplicity of construction against the deficits in performance, the boomless X LPA yields an honest debate, whereas the boomless trapezoidal array performed too poorly to contemplate its use.

A Larger X LPA with Boom from Amateur Literature

Rothammels Antennenbuch contains not only a trapezoidal zig-zag array for potential home replication, but as well 2 X LPAs. Unfortunately, each array uses a different set of design parameters, so we can only sample their performance individually. **Fig. 14** shows the outline of the larger of two X LPAs with central booms. The array uses 12 elements, which suggest a higher value of τ (0.84). Like the trapezoidal array that we examined in Part 2, the values of α' and of ψ are 60° and 45°, respectively. Also like the trapezoidal array, the shortest elements are close enough to the vertex the permit extensions of the final element and the boom to that point.

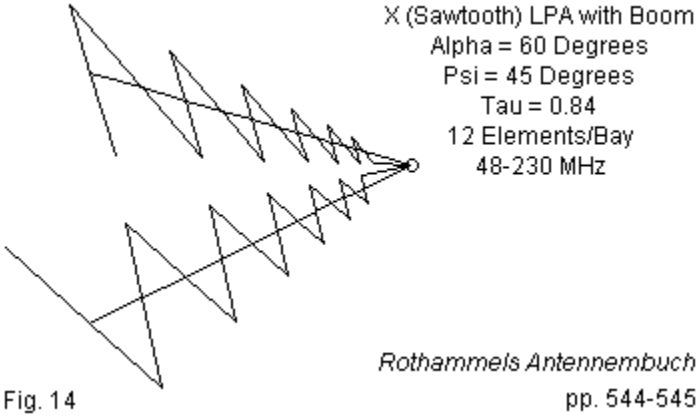

Fig. 14

The specified design range for the array was 48 to 230 MHz. However, calculations of the element locations appear to have used a minimum design frequency of 50 MHz. The dimensions appear in **Fig. 15** in a 2-part table. The lower section shows the calculation of the boom positions for the array. The models for this array used 2.54-mm (0.1") diameter lossless wire. **Table 5** samples the arrays performance at 50, 100, 150, and 200 MHz.

Table. 5. Sample performance values: 12 elements/bay, α = 60°, τ = 0.84, ψ = 45°

Frequency MHz	Max. Gain dBi	Front-Back Ratio dB	E BW degrees	H BW degrees	Impedance R +/- jX Ω	300-Ω SWR
50	5.64	3.09	72.9	92.2	375 – j458	3.64
100	8.49	11.88	67.8	74.0	294 + j 41	1.15
150	8.44	10.51	63.8	73.4	380 + j 0	1.27
200	8.69	11.50	63.2	74.6	225 - j 28	1.36

Although the trapezoidal amateur array that we looked at in Part 2 showed relatively smooth gain and front-to-back performance for the entire passband, the X LPA shows a serious deficit at the lowest sampled frequency. Moreover, the feedpoint impedance at this frequency shows a very high reactive component, raising the 300-Ω SWR value to uncomfortably high levels. Above the lowest frequency, the performance levels out at gain values only about 1 dB lower

than the X LPA using a τ of 0.9. However, the front-to-back values correspond only to those we might obtain from a 2-element driver-reflector Yagi.

Zig-Zag Log-Periodic Antenna Elements											Fig. 15
DARC Large X-LPA		p. 544									
Work Sheet		**Bold = User Entry**									
Tau		**0.840**								Sigma	0.069
Alpha	degrees	**60.00**	degrees	1.047	radians	1/2Alpha	0.524	tanAlpha	0.5774		0.069
F-low		**50.00**	MHz								
F-high		**200.00**	MHz								
L-long		3.00	meters	9.84	feet	118.11	inches				
Lhigh		0.75	meters	2.46	feet	29.53	inches				
L*1.6		0.47	meters	1.54	feet	18.45	inches				
Rv	Vertex R	2.60	meters	8.52	feet	102.29	inches				
Element	Ln	Ln/2	Rn	Element	Lfeet	Lft/2	Rfeet	Element	Linch	Lin/2	Rinch
1	3.000	1.500	2.598	*1*	9.84	4.92	8.52	*1*	118.11	59.06	102.29
2	2.520	1.260	2.182	*2*	8.27	4.13	7.16	*2*	99.21	49.61	85.92
3	2.117	1.058	1.833	*3*	6.94	3.47	6.01	*3*	83.34	41.67	72.17
4	1.778	0.889	1.540	*4*	5.83	2.92	5.05	*4*	70.00	35.00	60.63
5	1.494	0.747	1.294	*5*	4.90	2.45	4.24	*5*	58.80	29.40	50.93
6	1.255	0.627	1.087	*6*	4.12	2.06	3.56	*6*	49.40	24.70	42.78
7	1.054	0.527	0.913	*7*	3.46	1.73	2.99	*7*	41.49	20.75	35.93
8	0.885	0.443	0.767	*8*	2.90	1.45	2.52	*8*	34.85	17.43	30.18
9	0.744	0.372	0.644	*9*	2.44	1.22	2.11	*9*	29.28	14.64	25.35
10	0.625	0.312	0.541	*10*	2.05	1.02	1.77	*10*	24.59	12.30	21.30
11	0.525	0.262	0.454	*11*	1.72	0.86	1.49	*11*	20.66	10.33	17.89
12	0.441	0.220	0.382	*12*	1.45	0.72	1.25	*12*	17.35	8.68	15.03
13	0.370	0.185	0.321	*13*	1.21	0.61	1.05	*13*	14.58	7.29	12.62

X-LPA Boom Calculations			
Adjacent	2.76		
Opposite	0.415692		
tanBeta	0.150613		
Rbm-n	2.372157		
Boom	Rbm-m	Rbm-ft	Rbm-in
1-2	2.372	7.78	93.39
2-3	1.993	6.54	78.45
3-4	1.674	5.49	65.90
4-5	1.406	4.61	55.35
5-6	1.181	3.87	46.50
6-7	0.992	3.25	39.06
7-8	0.833	2.73	32.81
8-9	0.700	2.30	27.56
9-10	0.588	1.93	23.15
10-11	0.494	1.62	19.45
11-12	0.415	1.36	16.33
12-13	0.349	1.14	13.72

Table 6. Frequency sweep summary: 50-200 MHz: 8 elements/bay, α = 60°, τ = 0.84, ψ = 45°

Category	Minimum	Maximum	Δ	Average
Gain dBi	5.64	9.24	3.60	8.35
Front-Back dB	3.09	12.38	9.29	10.46
E Beamwidth °	59.1	74.4	15.3	67.5

The sweep summary in **Table 6** reveals the same set of impressions. Still, among arrays with high values of ψ and α', the array does show relatively smooth E-plane patterns without too much variation in the beam width. However, as **Fig. 16** makes clear, the array exhibits less control over the rearward lobe structure. In terms of 1970-era television reception, the antenna would be subject to interference from distant stations anywhere within the rearward quadrants.

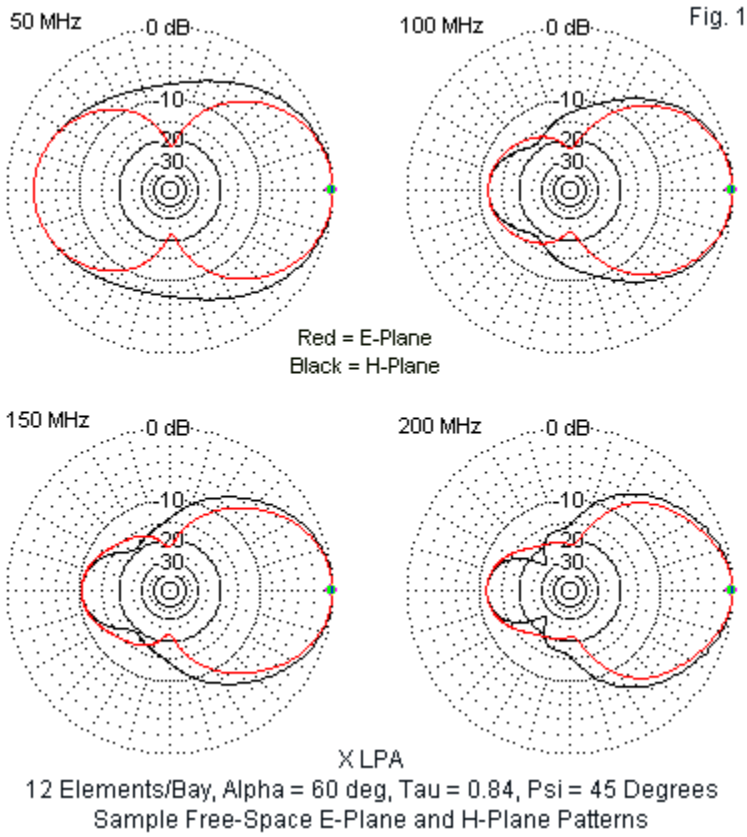

Fig. 16

X LPA
12 Elements/Bay, Alpha = 60 deg, Tau = 0.84, Psi = 45 Degrees
Sample Free-Space E-Plane and H-Plane Patterns

The sweep graphs in **Fig. 17** and **Fig. 18** confirm the tabular information. Note that the performance drop near the lower end of the passband begins at a higher frequency than the impedance deficit, a property that we have seen in other X LPAs.

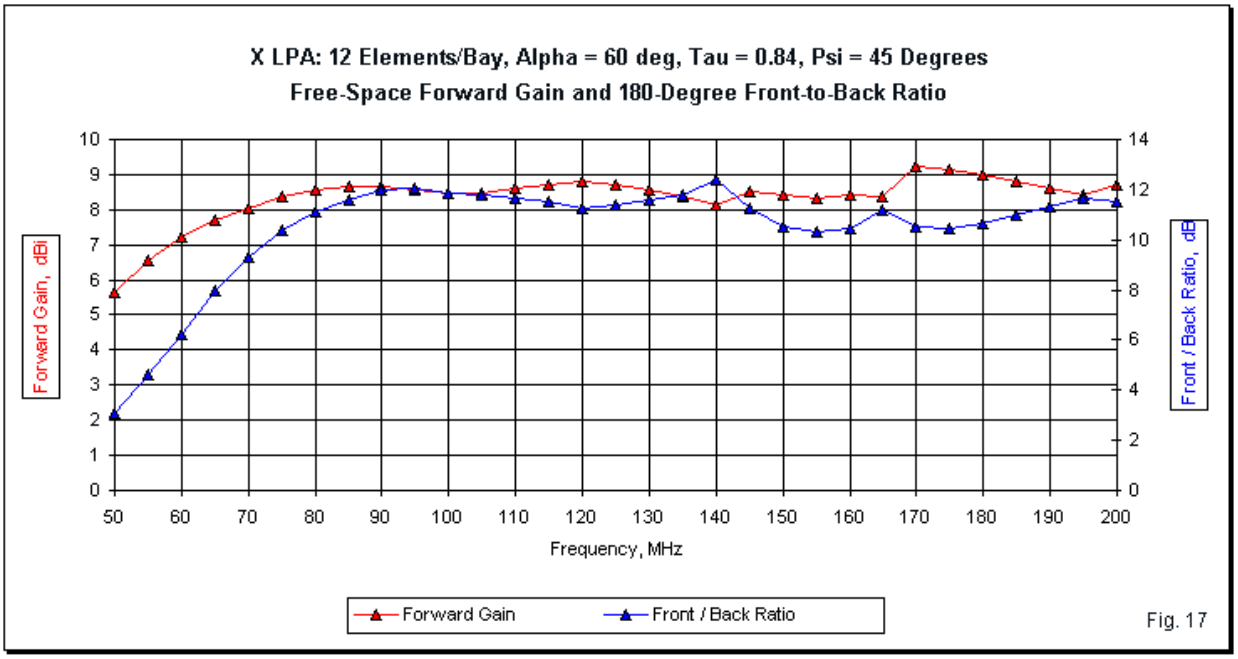

Fig. 17

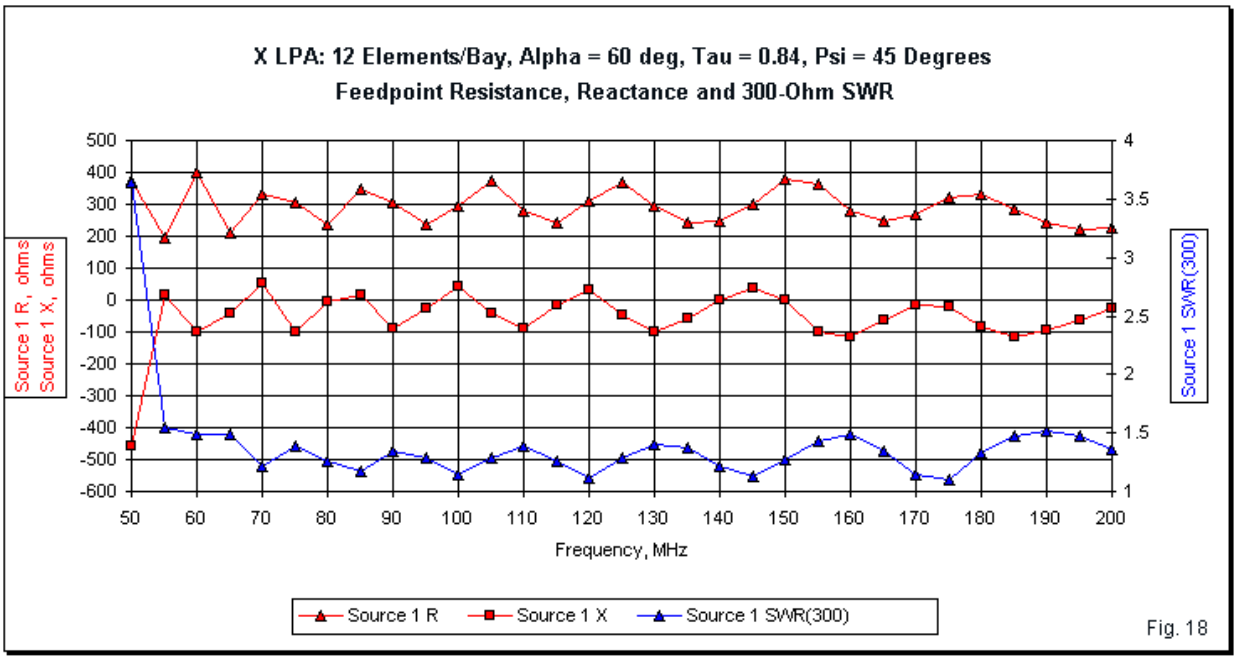

A Smaller X LPA with Boom from Amateur Literature

Rothamel also presents a smaller X LPA that uses only 8 elements, with a τ of 0.707. The ψ-angle remains a standard 45°. The listed value of α' was 75°, but I had to reduce the angle to 70° to bring the listed dimensions into coincidence with standard calculations of element dimensions. **Fig. 19** shows the outline of the array.

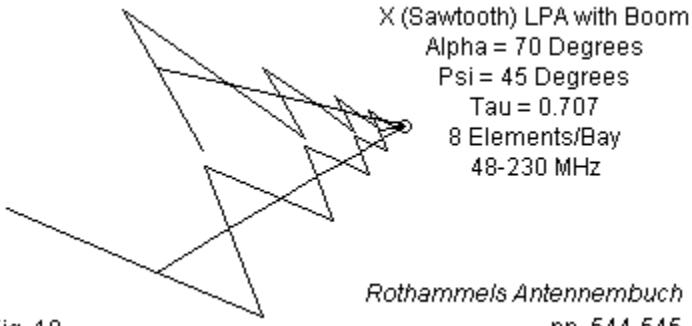

The dimensions used in the model appear in **Fig. 20**, which again has an upper and a lower section. The lower portion shows the relevant boom calculations. Like the larger X LPA, the smaller version draws the end of the shortest element and the boom all the way to the vertex. The distance is fairly short, as indicated by the smallest value of Rn in the dimension table.

Table 7 and **Table 8** present the performance sampling information and the sweep data summary, respectively. The performance deficiencies at the low end of the passband once more stand out in both tables. The one interesting category is the 200-Ω SWR value set. The small array manages to maintain values that are less than 2:1 at all sampled frequencies. Once more, the X LPA impedance performance has broader-banded characteristics than the gain, although the SWR does rise a small amount above 2:1 at 2 points in the passband.

Zig-Zag Log-Periodic Antenna Elements											Fig. 20
DARC X-LPA-Small			p. 544								
Work Sheet		**Bold = User Entry**									
Tau		**0.707**								Sigma	0.105
Alpha	degrees	**70.00**	degrees	1.222	radians	1/2Alpha	0.611	tanAlpha	0.7002		0.105
F-low		**48.00**	MHz								
F-high		**230.00**	MHz								
L-long		3.13	meters	10.25	feet	123.03	inches				
Lhigh		0.65	meters	2.14	feet	25.68	inches				
L*1.6		0.41	meters	1.34	feet	16.05	inches				
Rv	Vertex R	2.23	meters	7.32	feet	87.85	inches				
Element	Ln	Ln/2	Rn	Element	Lfeet	Lft/2	Rfeet	Element	Linch	Lin/2	Rinch
1	3.125	1.563	2.231	*1*	10.25	5.13	7.32	*1*	123.03	61.52	87.85
2	2.209	1.105	1.578	*2*	7.25	3.62	5.18	*2*	86.98	43.49	62.11
3	1.562	0.781	1.115	*3*	5.12	2.56	3.66	*3*	61.50	30.75	43.91
4	1.104	0.552	0.789	*4*	3.62	1.81	2.59	*4*	43.48	21.74	31.05
5	0.781	0.390	0.558	*5*	2.56	1.28	1.83	*5*	30.74	15.37	21.95
6	0.552	0.276	0.394	*6*	1.81	0.91	1.29	*6*	21.73	10.87	15.52
7	0.390	0.195	0.279	*7*	1.28	0.64	0.91	*7*	15.37	7.68	10.97
8	0.276	0.138	0.197	*8*	0.91	0.45	0.65	*8*	10.86	5.43	7.76
9	0.195	0.098	0.139	*9*	0.64	0.32	0.46	*9*	7.68	3.84	5.48

X-LPA Boom Calculations			
Adjacent	2.667188		
Opposite	0.653824		
tanBeta	0.245136		
Rbm-n	1.848456		
Boom	Rbm-m	Rbm-ft	Rbm-in
1-2	1.848	6.06	72.77
2-3	1.307	4.29	51.45
3-4	0.924	3.03	36.38
4-5	0.653	2.14	25.72
5-6	0.462	1.52	18.18
6-7	0.327	1.07	12.86
7-8	0.231	0.76	9.09
8-9	0.163	0.54	6.43

Table. 7. Sample performance values: 8 elements/bay, α = 70°, τ = 0.707, ψ = 45°

Frequency MHz	Max. Gain dBi	Front-Back Ratio dB	E BW degrees	H BW degrees	Impedance R +/- jX Ω	200-Ω SWR
50	4.09	1.75	75.7	134.0	203 – j112	1.73
100	6.96	10.73	66.8	89.6	223 + j 7	1.12
150	6.32	9.90	80.8	105.8	260 + j 28	1.33
200	6.92	9.67	79.4	99.6	209 - j 38	1.21

Table 8. Frequency sweep summary: 50-200 MHz: 8 elements/bay, α = 70°, τ = 0.707, ψ = 45°

Category	Minimum	Maximum	Δ	Average
Gain dBi	4.09	7.20	3.11	6.37
Front-Back dB	1.75	12.45	10.70	8.69
E Beamwidth °	64.0	80.8	16.8	70.9

As we might expect from such a sparsely populated array, pattern control decays more significantly than we found in the larger amateur X LPA. As shown in **Fig. 21**, the rearward lobes of the array at all sampled frequencies allow for considerable interference from the rear. The E-plane beamwidth values are close to those that are typical of a simple dipole.

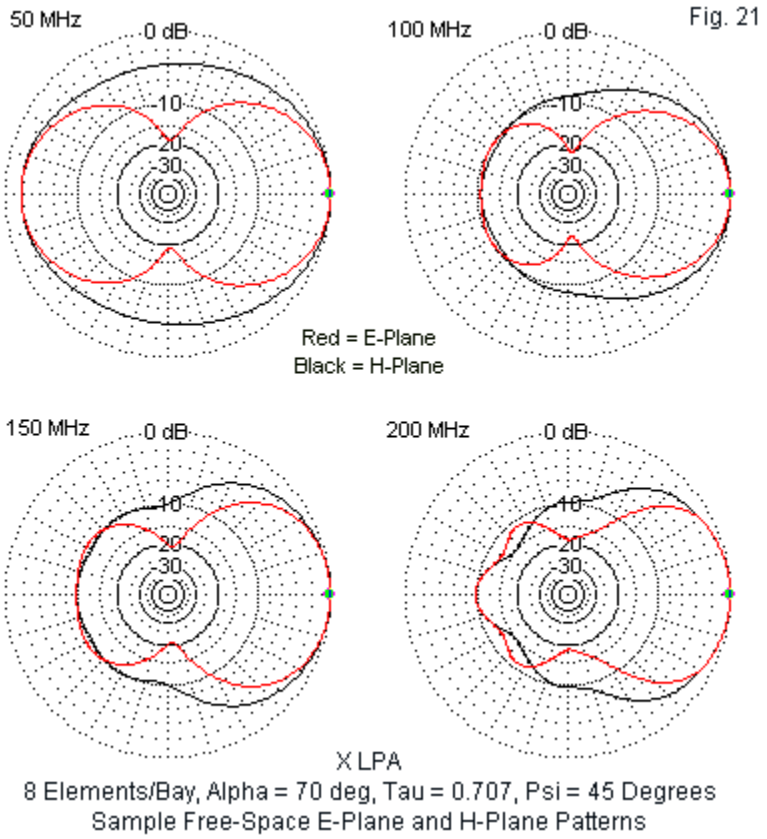

Fig. 21

Fig. 22 and **Fig. 23** provide sweep graphs that correlate with the tabular information. The gain and front-to-back graph is notable for two reasons. First, the performance curves are subject to sudden changes. Second, the low-end performance deficiencies cover a wider portion of the total passband.

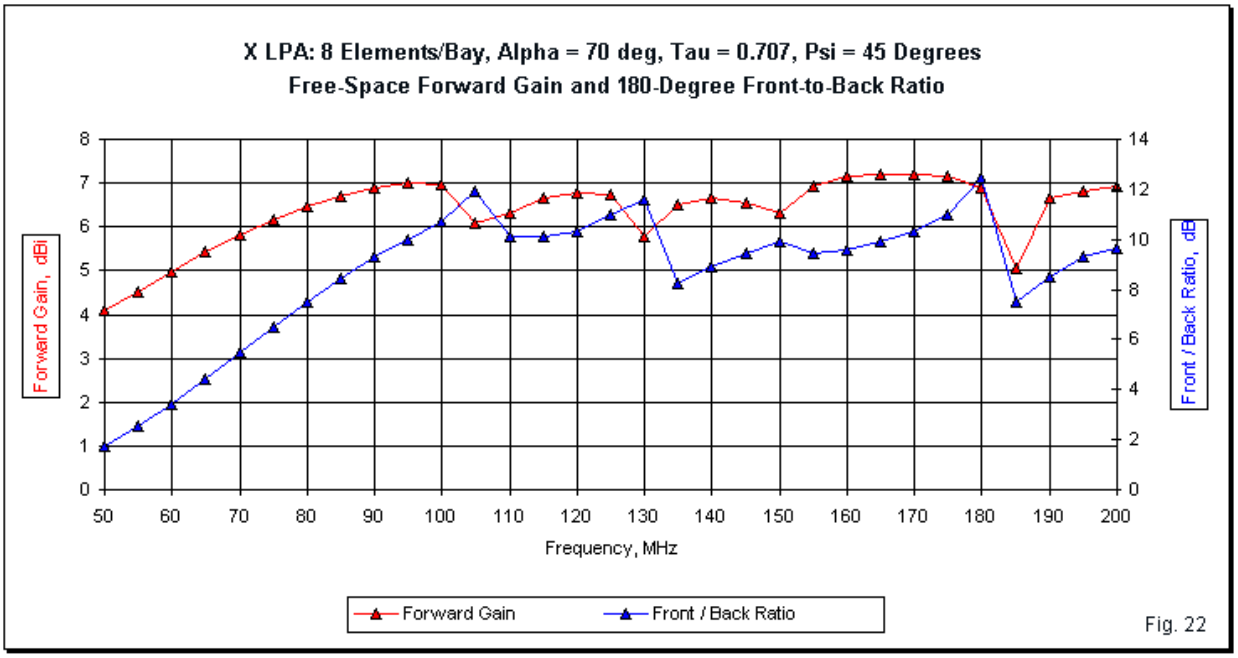

Fig. 22

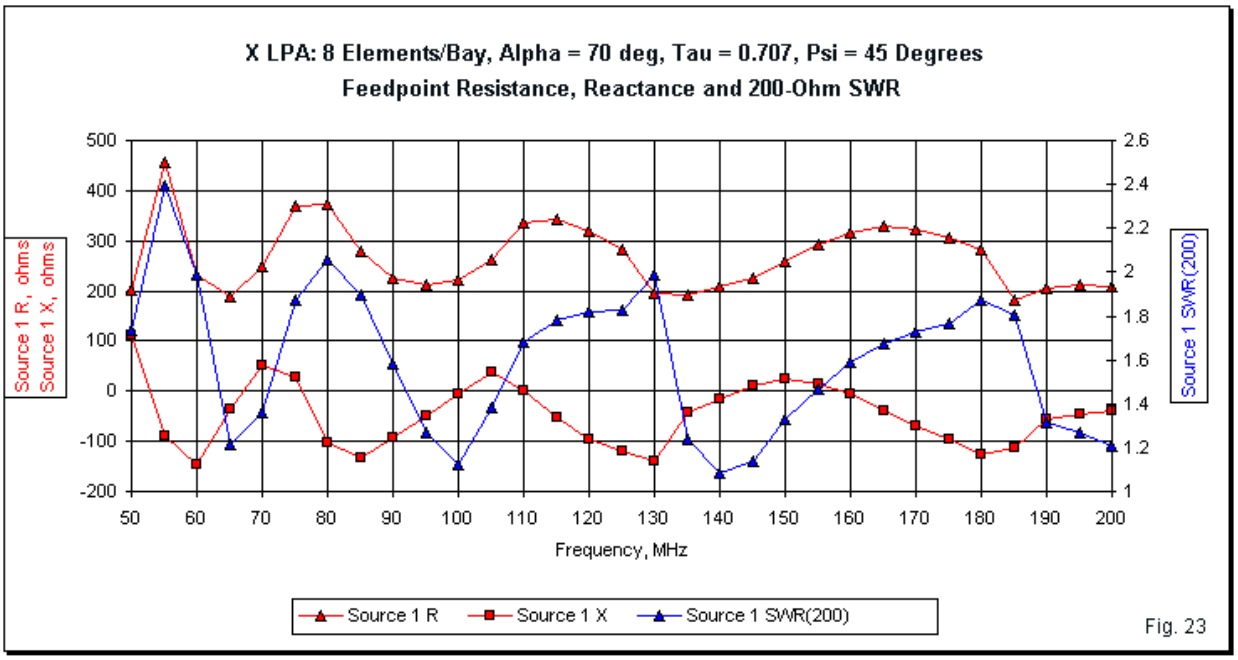

The impedance graph reveals that the small X LPA undergoes more radical changes in both resistance and reactance than the larger array. As well, we can easily find the SWR excursions above 2:1 at 55 and 80 MHz, with a borderline case at 130 MHz.

Of the two old-style X LPA designs, only the larger version might pass muster for adequate wide-band performance by 21st century standards—and then, only if we correct the deficiencies at the lower end of the passband. While we make those corrections, we might also experiment with the optimum value for the ψ-angle and not blithely accept the 45° standard that was common when these designs emerged.

Conclusion

Our main goal in all three parts of this exercise has been to compare the performance of "standard" LPDA design against zig-zag LPA designs that came earlier. To level of field of comparison, we used a fixed set of design parameters for all of our candidate designs: $\tau = 0.9$, $\sigma = 0.167$, $\alpha' = 17°$. All arrays used 20 0.1"-diameter elements per bay. Since the zig-zag designs required experimental selection of the ψ-angle, we let that factor be a variable.

Virtually none of the configurations showed exceptionless performance across the entire passband, a condition that we created by limiting the compensatory steps normally used to define the operative dimensions. Some versions showed weakness at the low end of the operating range, while others saw declines nearer to the upper end. Virtually all of the designs (with the exception of the boomless trapezoidal array) are subject to relatively easy reworking to correct the deficiencies, but the result will be as many different designs as we have types of LPAs.

Along the way, we have made some relevant comparisons between and among configurations. Repeating those textual assertions might leave their foundations uncertain. Therefore, by way of final summary, I have created **Table 9**, a compilation of the sweep summaries of the representative arrays of all types covered in these notes. The data allow you

to draw your own conclusions. For further data on variations of each LPA type, see the data appendix.

Table 9. Sweep data summary, 50-200 MHz in 5-MHz increments

LPDA, single-bay

Category	Minimum	Maximum	Δ	Average
Gain dBi	7.33	8.52	1.19	8.09
Front-Back dB	16.71	44.56	27.85	28.93
E Beamwidth °	60.8	66.4	5.6	63.7

Double-bay, Ψ=10°

Category	Minimum	Maximum	Δ	Average
Gain dBi	9.35	10.79	1.18	10.00
Front-Back dB	14.28	63.75	49.47	35.93
E Beamwidth °	54.0	61.0	7.0	57.8

Trapezoidal zig-zag LPA, with boom, ψ = 5°

Category	Minimum	Maximum	Δ	Average
Gain dBi	7.71	8.57	0.86	8.35
Front-Back dB	20.13	32.04	11.91	27.12
E Beamwidth °	63.0	68.8	5.8	65.0

Trapezoidal zig-zag LPA, without boom, Ψ = 20°

Category	Minimum	Maximum	Δ	Average
Gain dBi	4.48	8.20	3.72	6.57
Front-Back dB	4.46	13.60	9.14	9.94
E Beamwidth °	73.6	170.0	96.4	109.7

X zig-zag LPA, with boom, ψ = 5°

Category	Minimum	Maximum	Δ	Average
Gain dBi	7.64	8.84	1.20	8.64
Front-Back dB	11.96	30.93	18.97	26.87
E Beamwidth °	62.4	64.6	2.2*	63.5

X zig-zag LPA, without boom, ψ =10°

Category	Minimum	Maximum	Δ	Average
Gain dBi	6.00	7.90	1.90	7.30
Front-Back dB	9.44	19.78	10.34	16.31
E Beamwidth °	73.0	107.6	34.6	84.0